

# Syntheses, Binding Properties, and Structures of Seven New Hemicarcerands Each Composed of Two Bowls Bridged by Three Tetramethylenedioxy Groups and a Fourth Unique Linkage<sup>1,2</sup>

Juyoung Yoon, Chimin Sheu, K. N. Houk, Carolyn B. Knobler, and Donald J. Cram\*

Department of Chemistry and Biochemistry, University of California at Los Angeles, Los Angeles, California 90095

Received July 8, 1996<sup>®</sup>

Treatment of 2 mol of the bowl-shaped tetrol **1** (derived originally from resorcinol and dihydrocinamaldehyde) with 3 mol of TsO(CH<sub>2</sub>)<sub>4</sub>OTs gave diol **2**. Eight compounds with different combinations of bridges were formed from **2** by treatment with Cs<sub>2</sub>CO<sub>3</sub> and the following reagents in the presence of potential guests to give either free or complexed hemicarcerands as follows: ClCH<sub>2</sub>Br gave **4**; TsO(CH<sub>2</sub>)<sub>2</sub>OTs gave **5**; TsO(CH<sub>2</sub>)<sub>3</sub>OTs gave **6**; MsO(CH<sub>2</sub>)<sub>4</sub>OMs gave **7**, a known system; MsO(CH<sub>2</sub>)<sub>5</sub>OMs gave **8**; 2,3-bis(bromomethyl)quinoxaline gave **9**; 1,3-(ClCH<sub>2</sub>)<sub>2</sub>C<sub>6</sub>H<sub>4</sub> gave **10**; 2,6-bis(chloromethyl)pyridine gave **11**. Thirty-six fully characterized new hemicarceplexes are reported which were prepared either directly from diol **2** by the “sealing in” of the guest during introduction of the fourth bridge, or by guest exchange driven by mass law at 25 to 160 °C. The guests ranged in size from CHCl<sub>3</sub> to 1,2,3-(MeO)<sub>3</sub>C<sub>6</sub>H<sub>3</sub>. The incarcerated guests correlated with portal sizes of their hosts. Crystal structures of **8**⊙4-MeC<sub>6</sub>H<sub>4</sub>OMe and **10**⊙CHCl<sub>3</sub> were determined. Changes in chemical shifts in <sup>1</sup>H NMR spectra of incarcerated and free guests are interpreted in terms of their locations in the hosts’ inner phases. The length and nature of the unique host bridge affects the chemical shifts of the other bridges. Force field calculations of structural models for *N*-methylpyrrolidinone incarcerated in **4**–**7** were made. Approximate half-lives for decomplexation were determined for complexes involving the larger hosts and guests. Force-field calculations were made of binding energies and activation energies for decomplexations of models of **7**⊙*N*-methylpyrrolidinone, **8**⊙*N*-methylpyrrolidinone, and **10**⊙*N*-methylpyrrolidinone. The activation energies for decomplexation were dissected into intrinsic and constrictive components.

## Introduction

Prior publications on hemicarceplexes involved the assembly of many hosts by the four-fold bridging of two bowl-shaped cavitands such as **1** with groups, all four of which were the same. Variation in the lengths and sizes of these groups and the sizes of guests controls the propensity for complex formation and their stabilities in solution. Hemicarceplexes were prepared by guest-templation of the shell closures, or by heating empty hosts with potential guests as solvent. A third method involves heating hosts or unstable complexes with large excesses of new guests in high-boiling solvents whose molecules are too large to enter or occupy the inner phases of hosts.<sup>3</sup> A fourth method was described, in which **2** containing three (CH<sub>2</sub>)<sub>4</sub> bridging groups was prepared (30–40% yields) from **1**, making use of the fact that the rate of introducing the fourth bridge leading to the host is slower than those rates for the first three. The fourth bridge was introduced in the presence of large excesses of guests that, in certain cases, were too big or unstable to provide complexes made by the other three methods.<sup>4</sup> For example, **7**⊙O(CH<sub>2</sub>CH<sub>2</sub>)<sub>2</sub>NCHO was prepared from **2** and MsO(CH<sub>2</sub>)<sub>4</sub>OMs in (Me<sub>2</sub>N)<sub>3</sub>PO (HMPA) containing O(CH<sub>2</sub>CH<sub>2</sub>)<sub>2</sub>NCHO. This “sealing in of guest”

method of complexation had the additional synthetic advantage that the fourth bridge could be the same (leading to **7**<sup>4</sup>) or different than the first three, as in **4**–**6** and **8**–**11**. In this manner **3** was prepared, which was found to complex potassium picrate, the picrate ion being incarcerated but the K<sup>+</sup> being ligated by the six oxygens of the fourth bridge.<sup>4</sup>

We report here the syntheses and study of new host systems **4**–**6** and **8**–**11** from diol **2** and appropriate dihalides, ditosylates, or dimesylates in the presence of Cs<sub>2</sub>CO<sub>3</sub> and potential guests.

## Results and Discussion

**Syntheses.** Diol **2** was prepared in 40% yield from **1** and 3 equiv of MsO(CH<sub>2</sub>)<sub>4</sub>OMs in a mixture of Cs<sub>2</sub>CO<sub>3</sub> and NMP<sup>5</sup> at 25 °C for 18 h.<sup>3</sup> This material served as starting material for the syntheses of the seven new host systems in which the fourth bridge (*R* of **4**–**6**, **8**–**11**) differs from the three (CH<sub>2</sub>)<sub>4</sub> bridges of **2**. Chart 1 summarizes the reagents, reaction conditions, solvents, product structures, and yields for these shell closures. The four aprotic dipolar solvents used were NMP,<sup>5</sup> DMSO, DMA,<sup>5</sup> and HMPA. Bridge donor groups and products were as follows: CH<sub>2</sub>BrCl led to **4**⊙NMP, **4**⊙DMSO, and **4**⊙DMA; TsOCH<sub>2</sub>CH<sub>2</sub>OTs gave **5**⊙NMP, **5**⊙DMSO, and **5**⊙DMA; TsO(CH<sub>2</sub>)<sub>3</sub>OTs provided **6**⊙NMP, **6**⊙DMSO, **6**⊙DMA, and empty **6** (HMPA as solvent); MsO(CH<sub>2</sub>)<sub>4</sub>OMs gave **7**<sup>6</sup> (HMPA as solvent); MsO(CH<sub>2</sub>)<sub>5</sub>-

<sup>®</sup> Abstract published in *Advance ACS Abstracts*, November 15, 1996.

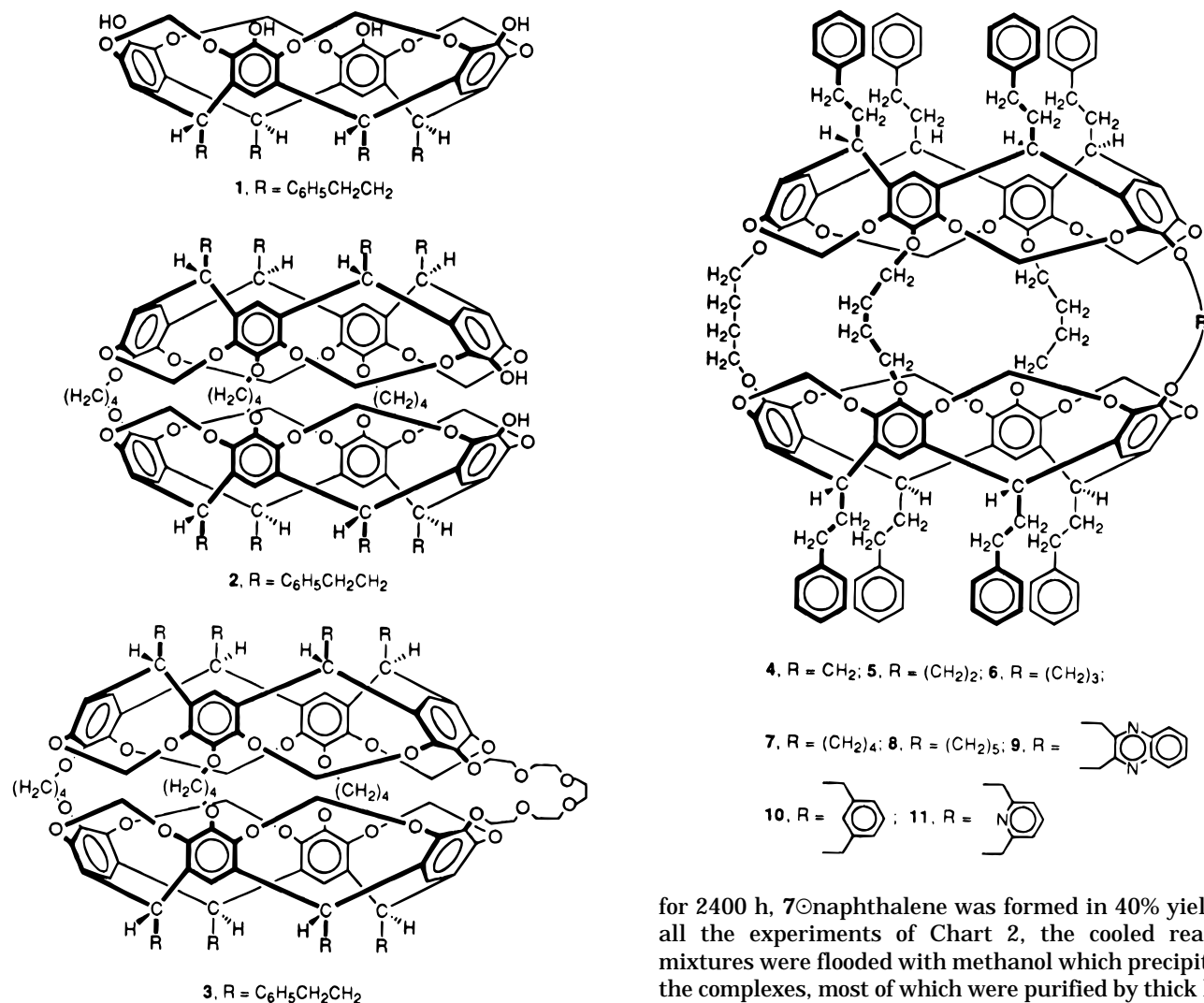
(1) Host–Guest Complexation 67.

(2) We warmly thank the U. S. Public Health Service for supporting grant GM-12640, and Dr. Kurt Loening for assistance with nomenclature.

(3) Cram, D. J.; Cram, J. M. *Container Molecules and Their Guests*. In *Monographs in Supramolecular Chemistry*; Stoddart, J. F., Ed.; Royal Society of Chemistry: Thomas Graham House, Science Park, Cambridge, U.K., 1994; pp 131–216.

(4) Kurdistan, S. K.; Helgeson, R. C.; Cram, D. J. *J. Am. Chem. Soc.* **1995**, *117*, 1659–1660.

(5) NMP stands for *N*-methylpyrrolidinone; DMA for (CH<sub>3</sub>)<sub>2</sub>-NCOCH<sub>3</sub>. GB/SA is the Generalized Born radii (GB)/solvent-accessible surface area (SA), an empirical solvation model. It is a semianalytical treatment of solvation and provides a volume-based continuum model for the electrostatic (polarization) component.<sup>13</sup>



OMs in NMP probably initially produced  $8\text{O}NMP$ , whose NMP was replaced with  $CHCl_3$  to give  $8\text{O}CHCl_3$  (stable to manipulation) during chromatographic purification with  $CHCl_3$  as the mobile phase; 2,3-bis(bromomethyl)quinoxaline provided  $9\text{O}NMP$ ,  $9\text{O}DMSO$ , and  $9\text{O}1,4-(MeO)_2C_6H_4$  (HMPA as solvent containing a 100:1 molar ratio of guest 1,4-(MeO) $_2C_6H_4$  to **2**). This last reaction, carried out at 24–50 °C, exemplifies the “sealing in” of a relatively large guest during introduction of the fourth bridge. With *m*-xylyl dichloride in NMP, whatever  $10\text{O}NMP$  was produced initially went to  $10\text{O}CHCl_3$  during isolation. Similarly, 2,6-bis(chloromethyl)pyridine ultimately gave  $11\text{O}CHCl_3$  although the shell closure was conducted in NMP. The temperatures for the shell closures varied from 24–75 °C, and the times from 48–53 h.

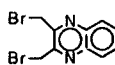
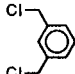
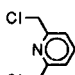
Chart 2 indicates the starting materials and products for the thermally induced formations of new hemicarcerplexes by either guest exchanges, or from empty host plus guests. Where possible, the new guest served as solvent for the starting empty host or complex. When necessary for solubility reasons  $Ph_2O$  or HMPA were used as solvents whose molecular volumes are too large to occupy the inner phases of any of these hosts. In such cases, guest-to-host molar ratios of at least 100 were employed. Temperatures and times for these equilibrations with one exception ranged respectively from 140–165 °C, with times of 72–96 h. The exception was when **7** and naphthalene dissolved in  $Ph_2O$  were heated at 200 °C

for 2400 h,  $7\text{O}naphthalene$  was formed in 40% yield. In all the experiments of Chart 2, the cooled reaction mixtures were flooded with methanol which precipitated the complexes, most of which were purified by thick layer chromatography with  $CHCl_3$  as the mobile phase. Complexes  $9\text{O}1,4-(MeO)_2C_6H_4$ ,  $10\text{O}4-MeC_6H_4OMe$ ,  $10\text{O}1,4-(MeO)_2C_6H_4$ , and  $11\text{O}4-MeC_6H_4OMe$  were used without chromatographic purification. With the exception of  $7\text{O}naphthalene$ , in which equilibrium was probably not established, the yields varied from 80–92%.

**Isolated Products Correlate with Portal Size.** Comparisons of CPK models suggest the inner volumes of these hosts differ very little from one another, but that the two portals that flank the last bridge introduced increase in size and conformational adaptivity in passing from **7** to **8**, and from **7** to **10** or **11**. The portals flanked by two  $(CH_2)_4$  groups already present in **2** are not greatly affected by the length of the fourth bridge. These two portals are invariant and composed of 26-membered rings, as compared to the other two portals that flank the fourth bridge. The latter vary in ring size with changes in the fourth bridge as follows: **4**, 23-membered rings; **5**, 24-membered rings; **6**, 25-membered rings; **7**, 26-membered rings; **8**, 27-membered rings; **9**, 26-membered rings with four bridging atoms coplanar; **10**, 27-membered rings with five of the bridging atoms coplanar; and **11**, 27-membered rings with five of the bridging atoms coplanar. To enter or exit the inner phase of these hosts, potential guests must pass through these rings, and for the guests studied, the larger portals are going to be the most used. With **4–7** and **9**, these are likely to be the original 26-membered portals; with **8**, **10**, and **11**, the larger portals are probably used.

**Chart 1. Fourth Bridge Donors React with Diol 2 To Give Either Host⊙Guest Complexes or Hosts When Heated in the Presence of Cs<sub>2</sub>CO<sub>3</sub>**

reaction media and source of guests

bridge-donor to 2	Conditions				Product				Conditions				Product				Conditions				Product				
	T (°)	t(h)	kind	ylid(%)	T (°)	t(h)	kind	ylid(%)	T (°)	t(h)	kind	ylid(%)	T (°)	t(h)	kind	ylid(%)	T (°)	t(h)	kind	ylid(%)	T (°)	t(h)	kind	ylid(%)	
	65	48	4⊙NMP	53	65	48	4⊙DMSO	51	65	48	4⊙DMA	54													
	75	48	5⊙NMP	45	75	48	5⊙DMSO	41	75	48	5⊙DMA	42													
	75	48	6⊙NMP	64	75	48	6⊙DMSO	60	75	48	6⊙DMA	64	75	48	6									46	
	25-60	72	7⊙NMP	55									25	48	7									60	
	25-50	53	8⊙CHCl <sub>3</sub> <sup>c</sup>	79																					
	24-50	53	9⊙NMP	78	24-50	53	9⊙DMSO	72					24-50	53	9⊙1,4-(MeO) <sub>2</sub> C <sub>6</sub> H <sub>4</sub> <sup>d</sup>	34									
	25-50	53	10⊙CHCl <sub>3</sub> <sup>c</sup>	81																					
	25-50	53	11⊙CHCl <sub>3</sub> <sup>c</sup>	77																					

<sup>a</sup> CPK examinations show that HMPA is too large to exist in the inner phases of these hosts.

<sup>b</sup> Taken from reference (4). From the same reference, 2 + MsO(CH<sub>2</sub>)<sub>4</sub>OMs in O(CH<sub>2</sub>CH<sub>2</sub>)<sub>2</sub>NCHO-Cs<sub>2</sub>CO<sub>3</sub> at 25 °C for 48 h gave 7⊙(CH<sub>2</sub>CH<sub>2</sub>)<sub>2</sub>NCHO (85%).

<sup>c</sup> During chromatographic isolation with CHCl<sub>3</sub>, host ⊙NMP exchanges guest to give host ⊙CHCl<sub>3</sub>, driven by mass law.

<sup>d</sup> HMPA which served as solvent contained a 100:1 molar ratio of 1,4-(MeO)<sub>2</sub>C<sub>6</sub>H<sub>4</sub>:2.

This analysis grossly correlates with observations incidental to the syntheses of the hosts. Thus the originally formed "sealed in" complexes of Chart 1 involving 4–7 and 9 survived their isolation in the presence of CHCl<sub>3</sub> during chromatography. Even empty 7 survived isolation without complexing CHCl<sub>3</sub>.<sup>4</sup> However, 8, 10, and 11 lost their putative original guest (NMP) during isolation in favor of complexing CHCl<sub>3</sub>. Models show little constrictive hindrance to the departure of NMP and entrance of CHCl<sub>3</sub> to the interior of these hosts. On the other hand, the slow complexation of naphthalene by empty 7 (2400 h to produce 40% complex at 200 °C) correlates with the fact that in CPK models complexation requires considerable modification of stable conformations and some bond angle adjustments in many parts of the host.

The numbers of non-hydrogen atoms in the guests introduced into hosts in this study ranges between 4 (CHCl<sub>3</sub>, (CH<sub>3</sub>)<sub>2</sub>SO) and 12 (1,2,3-(MeO)<sub>3</sub>C<sub>6</sub>H<sub>3</sub>), the most common guests containing 8 to 10 non-hydrogen atoms, six often in the form of a benzene ring. Host 7 in other studies was found to incarcerate 33 other guests of widely differing structures possessing most of the common functional groups, none of which contained more than 10 non-hydrogen atoms.<sup>6,7</sup> Those selected for the current study were chosen generally for their size, solubility properties, boiling points, simplicity of their <sup>1</sup>H NMR spectra, and probability of forming a hemiacarceplex. Almost all organic compounds containing 8 or less non-

hydrogen atoms are good candidate guests for the hosts of this study. However, it is highly probable that hosts 8, 10, and 11 are capable of incarcerating larger guests than 4–7 and 9, although the only example reported here is 10⊙1,2,3-(MeO)<sub>3</sub>C<sub>6</sub>H<sub>3</sub>.

**Crystal Structures of 8⊙4-MeC<sub>6</sub>H<sub>4</sub>OMe and 10⊙CHCl<sub>3</sub>.** Crystal structures of 8⊙4-MeC<sub>6</sub>H<sub>4</sub>OMe⊙2PhNO<sub>2</sub> (*R* = 0.162) and 10⊙CHCl<sub>3</sub>⊙2PhNO<sub>2</sub>⊙2PhNO<sub>2</sub> (*R* = 0.17) were determined.<sup>8</sup> Chart 3 provides both side and partial top stereoviews of the complexes. In the latter, the two sets of four oxygens that terminate the intermolecular bridges are connected by heavy lines to form two near planar squares attached to one another by the four interhemispheric bridges, the rest of the host being omitted. These top view partial structures both demonstrate that the carbons and hydrogens of the four bridges all lie outside the volume of a solid figure defined by the eight oxygens at its corners. This geometry reflects the fact that the unshared electron pairs of all eight oxygens face inward toward the cavity, and their bonds to the bridges must diverge from the cavity. This arrangement gives an *out-in-out* orientation of unshared electron pairs for the three oxygens attached to adjacent carbons on each of the eight benzene rings of the host, which provides for the greatest compensation of dipoles and lowest energy.







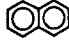
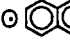
Crystalline 8⊙4-MeC<sub>6</sub>H<sub>4</sub>OMe⊙2PhNO<sub>2</sub> is isostructural with more than 25 hemiacarceplexes of 7⊙guest⊙

(6) Robbins, T. A.; Knobler, C. B.; Bellew, D. R.; Cram, D. J. *J. Am. Chem. Soc.* **1994**, *116*, 111–122.

(7) Robbins, T. A.; Cram, D. J. *J. Am. Chem. Soc.* **1993**, *115*, 12199–12200.

(8) The authors have deposited atomic coordinates for these structures with the Cambridge Crystallographic Data Center. The coordinates can be obtained, on request, from the Director, Cambridge Crystallographic Data Centre, 12 Union Road, Cambridge, CB2 1EZ, UK.

**Chart 2. New Hemicarceplexes Prepared by Mass-Law Driven Guest Exchange or from Free Host-Complexing Solvent or Solutes, Both Methods at Elevated Temperature**

starting material	medium		conditions		product	
	solvent	solute	T (°C)	t (h)	kind	yield (%)
4⊙DMA	1,4-(Me) <sub>2</sub> C <sub>6</sub> H <sub>4</sub>		140	72	4⊙1,4-(Me) <sub>2</sub> C <sub>6</sub> H <sub>4</sub>	85
5⊙DMA	1,4-(Me) <sub>2</sub> C <sub>6</sub> H <sub>4</sub>		140	72	5⊙1,4-(Me) <sub>2</sub> C <sub>6</sub> H <sub>4</sub>	88
6	1,4-(Me) <sub>2</sub> C <sub>6</sub> H <sub>4</sub>		140	72	6⊙1,4-(Me) <sub>2</sub> C <sub>6</sub> H <sub>4</sub>	90
7	Ph <sub>2</sub> O <sup>a</sup>		200	2400	7⊙ 	40 <sup>b</sup>
7 <sup>c</sup>	C <sub>6</sub> H <sub>5</sub> OCH <sub>2</sub> CH=CH <sub>2</sub>		160	96	7⊙C <sub>6</sub> H <sub>5</sub> OCH <sub>2</sub> CH=CH <sub>2</sub>	90
8	CHCl <sub>2</sub> CHCl <sub>2</sub>		140	72	8⊙CHCl <sub>2</sub> CHCl <sub>2</sub>	92
8⊙CHCl <sub>3</sub>	Ph <sub>2</sub> O <sup>a</sup>		165	72	8⊙ 	84
8⊙CHCl <sub>3</sub>	Ph <sub>2</sub> O <sup>a</sup>	1,4-(MeO) <sub>2</sub> C <sub>6</sub> H <sub>4</sub>	165	72	8⊙1,4-(MeO) <sub>2</sub> C <sub>6</sub> H <sub>4</sub>	92
8⊙CHCl <sub>3</sub>	1,2-(MeO) <sub>2</sub> C <sub>6</sub> H <sub>4</sub>		165	72	8⊙1,2-(MeO) <sub>2</sub> C <sub>6</sub> H <sub>4</sub>	86
8⊙CHCl <sub>3</sub>	1,3-(MeO) <sub>2</sub> C <sub>6</sub> H <sub>4</sub>		165	72	8⊙1,3-(MeO) <sub>2</sub> C <sub>6</sub> H <sub>4</sub>	89
8⊙CHCl <sub>3</sub>	4-MeOC <sub>6</sub> H <sub>4</sub> Me		165	72	8⊙4-MeOC <sub>6</sub> H <sub>4</sub> Me	92
8⊙CHCl <sub>3</sub>	2-HOC <sub>6</sub> H <sub>4</sub> Me		165	72	8⊙2-HOC <sub>6</sub> H <sub>4</sub> Me	90
10⊙CHCl <sub>3</sub>	CHCl <sub>2</sub> CHCl <sub>2</sub>		140	72	10⊙CHCl <sub>2</sub> CHCl <sub>2</sub>	91
10⊙CHCl <sub>3</sub>	Ph <sub>2</sub> O <sup>a</sup>		165	72	10⊙ 	85
10⊙CHCl <sub>3</sub>	1,2-(MeO) <sub>2</sub> C <sub>6</sub> H <sub>4</sub>		165	72	10⊙1,2-(MeO) <sub>2</sub> C <sub>6</sub> H <sub>4</sub>	87
10⊙CHCl <sub>3</sub>	1,3-(MeO) <sub>2</sub> C <sub>6</sub> H <sub>4</sub>		165	72	10⊙1,3-(MeO) <sub>2</sub> C <sub>6</sub> H <sub>4</sub>	89
10⊙CHCl <sub>3</sub>	Ph <sub>2</sub> O <sup>a</sup>	1,4-(MeO) <sub>2</sub> C <sub>6</sub> H <sub>4</sub>	165	72	10⊙1,4-(MeO) <sub>2</sub> C <sub>6</sub> H <sub>4</sub>	90
10⊙CHCl <sub>3</sub>	4-MeOC <sub>6</sub> H <sub>4</sub> Me		165	72	10⊙4-MeOC <sub>6</sub> H <sub>4</sub> Me	90
10⊙CHCl <sub>3</sub>	Ph <sub>2</sub> O <sup>a</sup>	1,2,3-(MeO) <sub>3</sub> C <sub>6</sub> H <sub>3</sub>	165	72	10⊙1,2,3-(MeO) <sub>3</sub> C <sub>6</sub> H <sub>3</sub>	80
11⊙CHCl <sub>3</sub>	Ph <sub>2</sub> O <sup>a</sup>		165	72	11⊙ 	87
11⊙CHCl <sub>3</sub>	1,2-(MeO) <sub>2</sub> C <sub>6</sub> H <sub>4</sub>		165	72	11⊙1,2-(MeO) <sub>2</sub> C <sub>6</sub> H <sub>4</sub>	84
11⊙CHCl <sub>3</sub>	1,3-(MeO) <sub>2</sub> C <sub>6</sub> H <sub>4</sub>		165	72	11⊙1,3-(MeO) <sub>2</sub> C <sub>6</sub> H <sub>4</sub>	86
11⊙CHCl <sub>3</sub>	4-MeOC <sub>6</sub> H <sub>4</sub> Me		165	72	11⊙4-MeOC <sub>6</sub> H <sub>4</sub> Me	90

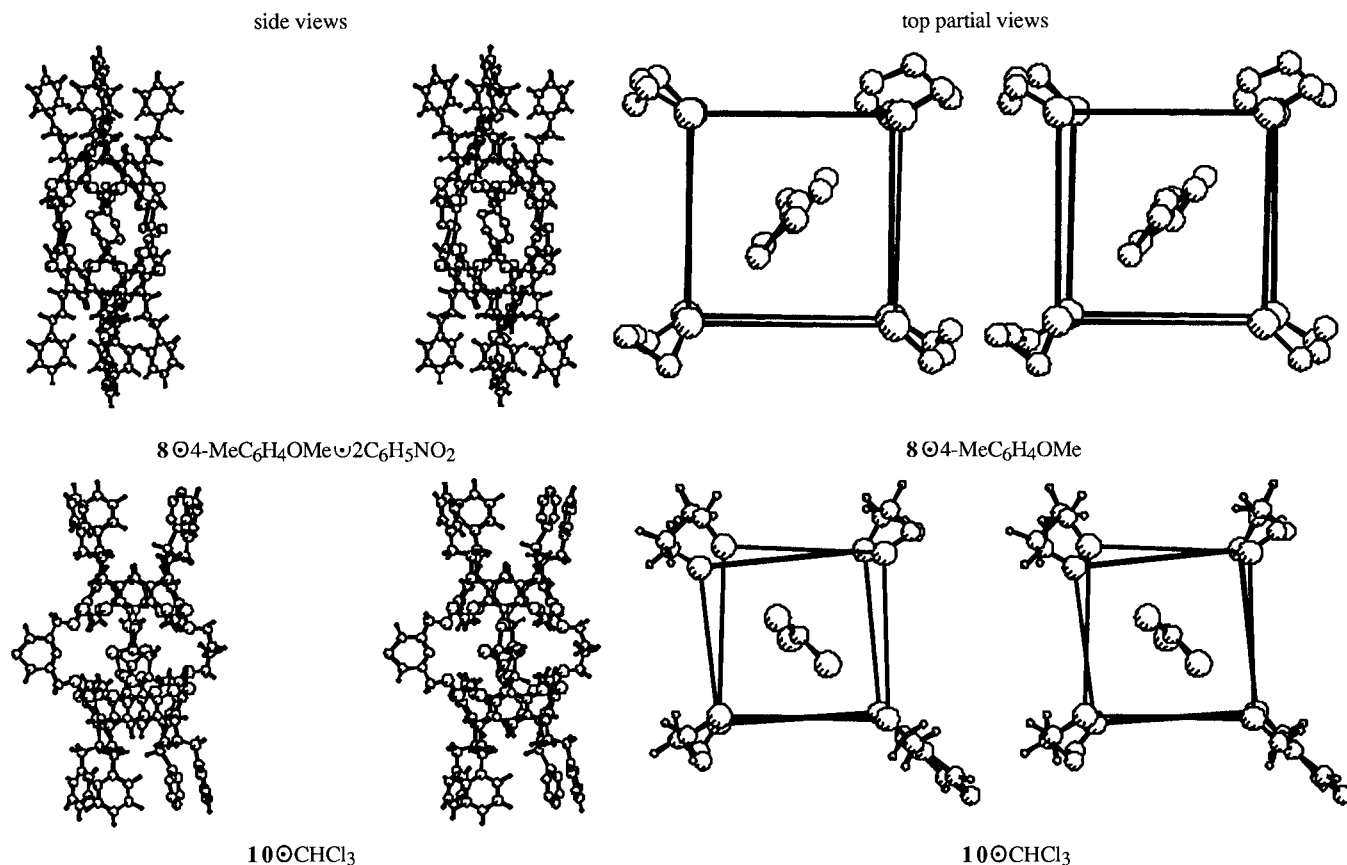
<sup>a</sup> (Me<sub>2</sub>N)<sub>3</sub>PO (HMPA) and Ph<sub>2</sub>O are each too large to occupy the interiors of these hosts. <sup>b</sup>The authors thank Siavash Kurdistani for this result. <sup>c</sup> Taken from reference (4).

2PhNO<sub>2</sub> containing four [O(CH<sub>2</sub>)<sub>4</sub>O] bridges, and therefore the parameters for the two cavitand moieties and for the two PhNO<sub>2</sub> molecules could be used to locate the guest, the three O(CH<sub>2</sub>)<sub>4</sub>O bridges, and the O(CH<sub>2</sub>)<sub>5</sub>O bridge. Because the complex is crystallographically centrosymmetric, the guest is required to be disordered. A "pair" of bridges is also required to have disorder (the unlike bridges related by the center of symmetry). The 4-MeC<sub>6</sub>H<sub>4</sub>OMe guest molecule in the host cavity is disordered because it lies on the crystallographic center of symmetry and is further disordered because it lies on either diagonal of the rectangular solid described by the eight terminal oxygens of the bridges as seen in the top partial stereoview. The four bridge-terminating oxygens attached to each bowl are coplanar within 0.01 (2) Å, and the planes are 4.10 Å distant from one another. These two planes are not rotated around the polar axis with respect to one another (see top view). The two PhNO<sub>2</sub> molecules are associated with the CH<sub>2</sub>CH<sub>2</sub>Ph "feet" attached to the northern and southern hemispheres, with

the nitro groups turned toward the globe of the host (see Chart 3, side view).

In the crystal structure of 10⊙CHCl<sub>3</sub>·2PhNO<sub>2</sub>·2PhNO<sub>2</sub>, the complex lies on a two-fold axis. The CHCl<sub>3</sub> is located in the cavity, but is disordered. Each set of four CH<sub>2</sub>CH<sub>2</sub>Ph groups surrounds a PhNO<sub>2</sub> molecule, with the nitro group turned toward the globe. The other two PhNO<sub>2</sub> molecules are interstitial. The PhNO<sub>2</sub> molecules are omitted from the drawings of Chart 3. The two sets of four oxygens that terminate the four inter-hemispheric bridges form two planes (± 0.02 (2) Å). The two planes miss being parallel to each other by 5.7°. The oxygen atoms of each interhemispheric bridge are distant from one another by the values (Å): OCH<sub>2</sub>C<sub>6</sub>H<sub>4</sub>CH<sub>2</sub>O, 4.47 (2); O(CH<sub>2</sub>)<sub>4</sub>O (flanking bridges), 4.02 (2) and 4.06 (2); O(CH<sub>2</sub>)<sub>4</sub>O (opposite bridge), 3.57 (2). The average distance between the two oxygen planes is 4.03 Å, less than the 4.10 Å distance in 8⊙4-MeC<sub>6</sub>H<sub>4</sub>OMe. The carbons and hydrogens of these four bridges all lie outside the solid defined by the eight apical oxygens. The two

Chart 3. Stereoviews of Crystal Structures of Hemicarceplexes



oxygen planes are slightly rotated and displaced from their best central axis with respect to one another. The top view of **10** shows that the two portals flanking the  $\text{OCH}_2\text{C}_6\text{H}_4\text{CH}_2\text{O}$  bridge are slightly more open than the two portals flanking the  $\text{O}(\text{CH}_2)_5\text{O}$  bridge in **8**. The long bridges are clearly visible at about 1 o'clock and 5 o'clock in the top views of **8** and **10**, respectively.

**Correlations between Guest Structures and Changes in Chemical Shifts of Incarcerated and Free Host Protons in  $^1\text{H}$  NMR Spectra.** Table 1 lists  $\delta$  for 12 guests dissolved in  $\text{CDCl}_3$ , 43 hemicarceplexes of these guests dissolved in  $\text{CDCl}_3$ , and  $\Delta\delta$  values for the guest protons ( $\Delta\delta = \delta_{\text{free}} - \delta_{\text{complexed}}$ ). In all cases except for the  $\text{OH}$  protons in **7**⊙**2-MeC<sub>6</sub>H<sub>4</sub>OH** and **8**⊙**2-MeC<sub>6</sub>H<sub>4</sub>OH** the  $\delta$  values moved upfield upon incarceration, due to the shielding effects of the faces of the eight aryl groups that line much of the surface of the inner phase. The  $\Delta\delta$  values range from a low of  $-0.76$  (in **8**⊙**2-MeC<sub>6</sub>H<sub>4</sub>OH**) to a high of  $4.41$  ppm (in **7**⊙**1,3-(MeO)<sub>2</sub>C<sub>6</sub>H<sub>4</sub>**).

Model examinations of **4**⊙**NMP**, **5**⊙**NMP**, **6**⊙**NMP**, **7**⊙**NMP**, and **9**⊙**NMP** indicate that the Me of the guest must occupy one of the polar, bowl-shaped interiors of the four hosts, and thus anchor the guest in the four hosts. The other protons of the  $\text{CH}_2\text{CH}_2\text{CH}_2$  parts of the guest are arranged in an arc which stretches like the handle of a tea kettle through the equator and past the other hemisphere of the inner phase to attach to the  $\text{C}=\text{O}$  (the spout of the tea kettle) whose axis points roughly toward the lower parts of the bridging groups of the hosts. Thus the  $\Delta\delta$  values of the four kinds of protons provide a sort of map of the shielding character of the different parts of the inner surfaces of the closely related hosts. The guest is presumed to rotate rapidly on the  $^1\text{H}$  NMR time scale around the axis of the  $\text{N}-\text{Me}$  bond, which is roughly coincident with the long polar axis of the host.

It also seems likely that  $\Delta\delta$  values should measure how far the Me protons are thrust into the shielding faces of the four aryls. Table 1 indicates the  $\Delta\delta$  values for the five  $\text{N}-\text{Me}$  protons decrease in the following order with *increases in the effective lengths* of the unique bridge of the host as follows:  $\text{CH}_2\text{C}=\text{CCH}_2$  (**9**),  $3.87$  ppm;  $\text{CH}_2$  (**4**),  $3.83$ ;  $\text{CH}_2\text{CH}_2$  (**5**),  $3.63$ ;  $\text{CH}_2\text{CH}_2\text{CH}_2$  (**6**),  $3.60$ ;  $\text{CH}_2\text{CH}_2\text{CH}_2\text{CH}_2$  (**7**),  $3.59$  ppm. By effective lengths, we mean the effect on the long axis of the inner phase of the hosts. Interestingly, the coplanarity requirement of the four-atom 2,3-dimethylenequinoxaline bridge of **9** forces it in CPK models to rotate about its  $C_2$  axis and thus act as a bridge even slightly shorter than the  $\text{CH}_2$  bridge of **4**. The effective lengths of the other four bridges fall in the expected order, with little difference between the  $(\text{CH}_2)_3$  and  $(\text{CH}_2)_4$  bridges. The  $\text{H}^b$  protons provide a similar sequence:  $\text{CH}_2\text{C}=\text{CCH}_2$ ,  $3.19$ ;  $\text{CH}_2$ ,  $3.13$ ;  $\text{CH}_2\text{CH}_2$ ,  $2.95$ ;  $\text{CH}_2\text{CH}_2\text{CH}_2$ ,  $2.83$ ;  $\text{CH}_2\text{CH}_2\text{CH}_2\text{CH}_2$ ,  $2.82$  ppm. The  $\text{H}^c$  protons give a somewhat different order:  $\text{CH}_2$ ,  $3.15$ ;  $\text{CH}_2\text{C}=\text{CCH}_2$ ,  $3.05$ ;  $\text{CH}_2\text{CH}_2$ ,  $2.79$ ;  $(\text{CH}_2)_3$ ,  $2.72$ ; and  $(\text{CH}_2)_4$ ,  $2.68$  ppm. The only distinguishable  $\text{H}^d$  protons were when the host bridges were  $\text{CH}_2\text{C}=\text{CCH}_2$  and  $\text{CH}_2$ , which gave the same  $\Delta\delta$  values ( $1.46$  ppm). As expected, for each complex, the three or four different protons available provided decreases in  $\Delta\delta$  values in the order  $\text{H}^a > \text{H}^b \approx \text{H}^c > \text{H}^d$ . In models, the  $\text{H}^c$  and  $\text{H}^d$  protons cannot penetrate as deeply into the polar regions of the hosts as can the  $\text{H}^a$  protons of the Me group.

The  $\Delta\delta$  values for  $\text{Me}_2\text{SO}$  (singlets) are smaller than those for  $\text{H}^a$  of NMP and vary much less with changes in the host's unique bridges, probably because this guest is smaller than NMP and less closely held. The order of  $\Delta\delta$  with changes in the unique bridges is as follows:  $\text{CH}_2\text{C}=\text{CCH}_2$ ,  $3.17$ ;  $\text{CH}_2$ ,  $3.14$ ;  $(\text{CH}_2)_3$ ,  $2.97$ ;  $(\text{CH}_2)_4$ ,  $2.95$ ;  $\text{CH}_2\text{CH}_2$ ,  $2.94$  ppm. Again, the *effective lengths* are the

**Table 1.** Effect of Host Structure on 500 MHz  $^1\text{H}$  NMR Spectra of Guests in  $\text{CDCl}_3$  at 25  $^\circ\text{C}$ 

Guest Structure	proton	free guest $\delta$	4 $\odot$ guest		5 $\odot$ guest		6 $\odot$ guest		7 $\odot$ guest		9 $\odot$ guest	
			$\delta$	$\Delta\delta$	$\delta$	$\Delta\delta$	$\delta$	$\Delta\delta$	$\delta$	$\Delta\delta$	$\delta$	$\Delta\delta$
	H <sup>a</sup>	2.70 (s)	-1.13 (s)	3.83	-0.93 (s)	3.63	-0.90 (s)	3.60	-0.89 (s)	3.59	-1.17 (s)	3.87
	H <sup>b</sup>	2.23 (t)	-0.90 (t)	3.13	-0.72 (t)	2.95	-0.60 (t)	2.83	-0.59 (t)	2.82	-0.96 (t)	3.19
	H <sup>c</sup>	1.90 (q)	-1.25 (q)	3.15	-0.89 (q)	2.79	-0.82 (q)	2.72	-0.78 (q)	2.68	-1.15 (q)	3.05
	H <sup>d</sup>	3.26 (t)	1.80 (t)	1.46	hidden	hidden	hidden	hidden	hidden	1.80 (t)	1.46	
	H <sup>a</sup>	2.46 (s)	-0.68 (s)	3.14	-0.48 (s)	2.94	-0.51 (s)	2.97	-0.49 (s)	2.95	-0.71 (s)	3.17
	H <sup>a</sup>	2.08 (s)	-1.92 (s)	4.00	-1.67 (s)	3.75	-1.68 (s)	3.76	-1.64 (s)	3.72		
	H <sup>b</sup>	3.02 (s)	-0.90 (s)	3.92	-0.56 (s)	3.58	-0.53 (s)	3.55	-0.42 (s)	3.44		
	H <sup>c</sup>	2.94 (s)	1.58 (s)	1.36	1.64 (s)	1.30	hidden		1.61 (s)	1.33		
	H <sup>a</sup>	2.32 (s)	-2.02 (s)	4.34	-1.93 (s)	4.25	-2.01 (s)	4.33	-2.08 (s)	4.40		
	H <sup>b</sup>	7.07 (s)	5.85 (s)	1.22	5.97 (s)	1.10	5.94 (s)	1.13	5.90 (s)	1.77		
	H <sup>a</sup>	5.95 (s)	4.75 (s)	1.20	4.29 (s)	1.66			4.35 (s)	1.60		
	H <sup>b</sup>	7.66 (d)	hidden		hidden				hidden		hidden	
	H <sup>a</sup>	7.30 (d)	3.09(br s)	4.21	3.36(br s)	3.94			3.35(br s)	3.95	3.37 (m)	3.93
	H <sup>a</sup>	3.77 (s)	-0.46 (s)	4.23	-0.41 (s)	4.18	-0.45 (s)	4.22	-0.38 (s)	4.15		
	H <sup>b</sup>	6.85 (s)	5.82 (s)	1.03	5.84 (s)	1.01	5.81 (s)	1.04	5.84 (s)	1.01		
	H <sup>a</sup>	3.80 (s)	-0.61 (s)	4.41	-0.55 (s)	4.35			-0.53 (s)	4.33	-0.50 (s)	4.30
	H <sup>b</sup>	6.50 (s)	5.42 (s)	1.08	5.48 (s)	1.02			5.48 (s)	1.02	5.49(br s)	1.01
	H <sup>c</sup>	6.54 (d)	4.82 (d)	1.72	5.02 (d)	1.52			5.03 (d)	1.51	5.00 (d)	1.54
	H <sup>d</sup>	7.20 (t)	4.12 (t)	3.08	hidden				hidden		hidden	
	H <sup>a</sup>	3.88 (s)	hidden		hidden				hidden		hidden	
	H <sup>b</sup>	6.9 (m)	hidden		5.46(br s)	1.4			5.45(br s)	1.5	5.55(br s)	1.3
	H <sup>c</sup>	6.9 (m)	4.98(br s)	1.9	hidden				hidden		hidden	
	H <sup>a</sup>	3.78 (s)	-0.35 (s)	4.13	-0.28 (s)	4.06			-0.26 (s)	4.04	-0.29 (s)	4.07
	H <sup>b</sup>	6.81 (d)	5.87 (s)	0.94	5.84 (d)	0.97			5.87 (d)	0.94	5.78 (d)	1.03
	H <sup>c</sup>	7.09 (d)	5.87 (s)	1.22	5.95 (d)	1.14			6.01 (d)	1.08	5.90 (d)	1.19
	H <sup>d</sup>	2.29 (s)	-2.11 (s)	4.40	-1.98 (s)	4.27			-1.96 (s)	4.25	-1.98 (s)	4.27
	H <sup>a</sup>	5.45 (s)	5.91 (s)	-0.46	6.21 (s)	-0.76						
	H <sup>b</sup>	2.31 (s)	-1.75 (s)	4.06	-1.68 (s)	3.99						
	H <sup>c</sup>	6.82 (d)	hidden		hidden							
	H <sup>d</sup>	6.92 (t)	6.13 (t)	0.79	6.14 (t)	0.78						
	H <sup>e</sup>	7.14 (t)	3.05 (t)	4.09	3.22 (t)	3.92						
	H <sup>f</sup>	7.18 (d)	5.73 (d)	1.45	5.98 (d)	1.20						
	H <sup>a</sup>	3.85 (s)							-0.41 (s)	4.26		
	H <sup>b</sup>	3.86 (s)							3.05 (s)	0.81		
	H <sup>c</sup>	6.58 (d)							hidden			
	H <sup>d</sup>	6.99 (d)							hidden			

shortest for the  $\text{CH}_2=\text{CCH}_2$  and  $\text{CH}_2$  bridges, but the other three  $\Delta\delta$  values do not vary significantly with the numbers of methylenes.

As observed for the carceplex of  $\text{MeCONMe}_2$  (DMA) whose host was identical to **4** except all four bridges were

$\text{CH}_2$ , the  $\text{H}^a$  and  $\text{H}^b$  methyls of DMA incarcerated in **4**–**7** give substantially higher  $\Delta\delta$  values (range 4.00–3.44 ppm) than the  $\text{H}^c$  methyls (range, 1.36–1.30 ppm). The  $\text{H}^a$  and  $\text{H}^b$  methyls lie on the long axis of DMA, which must be close to being coincident with the long axes of

the host cavities. Thus the H<sup>a</sup> and H<sup>b</sup> methyls are located in the two polar (most shielding) parts of the host's interior, and the H<sup>c</sup> methyls lie in the equatorial region of the bridges. The H<sup>a</sup> protons'  $\Delta\delta$  value is 4.00 with the shortest unique bridge (CH<sub>2</sub>), but decreases to 3.75, 3.76, and 3.72 ppm, respectively, as that bridge becomes CH<sub>2</sub>-CH<sub>2</sub>, (CH<sub>2</sub>)<sub>3</sub>, and (CH<sub>2</sub>)<sub>4</sub>. The H<sup>b</sup> protons'  $\Delta\delta$  values decrease more markedly and regularly with the lengthening of the unique bridge as follows: CH<sub>2</sub>, 3.92; CH<sub>2</sub>-CH<sub>2</sub>, 3.58; (CH<sub>2</sub>)<sub>3</sub>, 3.55; (CH<sub>2</sub>)<sub>4</sub>, 3.44 ppm. The equatorially-located H<sup>c</sup> protons provide  $\Delta\delta$  values that vary little and irregularly with bridge length.

In models, 1,4-Me<sub>2</sub>C<sub>6</sub>H<sub>4</sub> fits comfortably in **4**–**7** with each of the two methyl groups occupying one of the two hemispheric bowls with the long axes of host and guest being essentially coincident. The H<sup>a</sup> protons of these methyls exhibit  $\Delta\delta$  values that change relatively little with the unique bridge changes as follows: CH<sub>2</sub>, 4.34; CH<sub>2</sub>CH<sub>2</sub>, 4.25; (CH<sub>2</sub>)<sub>3</sub>, 4.33; (CH<sub>2</sub>)<sub>4</sub>, 4.40 ppm. The non-monotonic orders in some of these patterns probably reflect different degrees of rotation of the two hemispheres with respect to one another as the unique bridge lengths change, and the host adapts to the steric requirements of these relatively rigid guests. The hosts more than the guests have bond angle and conformational degrees of freedom that can vary cumulatively to minimize the energies of the complexes of **4**–**7** and **9**. The enlargement of the host's portal should be more temperature-sensitive than the compressibility of the guest.

Both host inner phases and guest volumes are larger for the complexes whose  $\Delta\delta$  values are reported in the bottom two-thirds of Table 1. The two protons (H<sup>a</sup>) of CHCl<sub>2</sub>CHCl<sub>2</sub> in models occupy niches defined by the much larger Cl atoms, and therefore cannot reach the inner shielding surfaces of the host when incarcerated. Accordingly, the  $\Delta\delta$  values for **7**, **8**, and **10** with unique bridges (CH<sub>2</sub>)<sub>4</sub>, (CH<sub>2</sub>)<sub>5</sub>, and 1,3-(CH<sub>2</sub>)<sub>2</sub>C<sub>6</sub>H<sub>4</sub> are 1.20, 1.66, and 1.60 ppm. In contrast, with naphthalene as guest, the protons are exposed, and in models of their complexes, the H<sup>b</sup> protons rest against the high-shielding faces of the northern and southern hemispheres of the host. Accordingly, the  $\Delta\delta$  values for H<sup>b</sup> are high and are as follows (unique bridges identify the host): (CH<sub>2</sub>)<sub>4</sub>, 4.21; (CH<sub>2</sub>)<sub>5</sub>, 3.94; 1,3-(CH<sub>2</sub>)<sub>2</sub>C<sub>6</sub>H<sub>4</sub>, 3.95; 2,6-(CH<sub>2</sub>)<sub>2</sub>pyridine, 3.93 ppm. As expected, the shortest unique bridge, (CH<sub>2</sub>)<sub>4</sub>, provides the highest  $\Delta\delta$  value.

The next three guests of Table 1 are the three isomeric dimethoxybenzenes. The most complementary relationship between host and guest with regard to the partners sharing the largest surface area is found in the complexes of **7**, **8**, **9**, and **10** with 1,4-(MeO)<sub>2</sub>C<sub>6</sub>H<sub>4</sub>. The H<sup>a</sup> methyl protons in models of the complexes are thrust nonsymmetrically into each of the two hemispheres of the hosts. Their  $\Delta\delta$  values are as follows: unique bridge (CH<sub>2</sub>)<sub>4</sub>, 4.23; (CH<sub>2</sub>)<sub>5</sub>, 4.18; CH<sub>2</sub>=CCH<sub>2</sub>, 4.22; and 1,3-(CH<sub>2</sub>)<sub>2</sub>C<sub>6</sub>H<sub>4</sub>, 4.15 ppm. The inner phases of these complexes appear to be very similar to one another in shape. More surprisingly, the same thing is observed for the 1,3-(MeO)<sub>2</sub>C<sub>6</sub>H<sub>4</sub> isomer. In models, the two methyls nicely fit into the two hemispheres of the host, which is consistent with the high  $\Delta\delta$  values for the H<sup>a</sup> protons of the two methyls, as follows: (CH<sub>2</sub>)<sub>4</sub>, 4.41; (CH<sub>2</sub>)<sub>5</sub>, 4.35; 1,3-(CH<sub>2</sub>)<sub>2</sub>C<sub>6</sub>H<sub>4</sub>, 4.33; and 2,6-(CH<sub>2</sub>)<sub>2</sub>pyridine, 4.30 ppm. In models, the H<sup>b</sup> proton is located in the equatorial region of the four complexes, and their  $\Delta\delta$  values range from 1.08 to 1.01 ppm. The H<sup>c</sup> protons'  $\Delta\delta$  values are somewhat higher, since they contact the edge of the aryl

faces, and their  $\Delta\delta$  values show the greatest range, 1.51 to 1.72 ppm. It is more difficult in models of complexes of 1,2-(MeO)<sub>2</sub>C<sub>6</sub>H<sub>4</sub> to locate the contacting parts since each OMe group inhibits its neighboring OMe group from penetrating the polar parts of the cavity. In none of the <sup>1</sup>H NMR spectra of the four complexes that were taken could the  $\delta$  values for the H<sup>a</sup> methyl protons be determined because of the overlap of host and guest signals. Probably a family of structures, nonequilibrating on the NMR time scale and close in energy, is responsible for the uninformative spectra.

Like 1,4-(MeO)<sub>2</sub>C<sub>6</sub>H<sub>4</sub> as guest, 4-MeOC<sub>6</sub>H<sub>4</sub>Me is highly complementary in shape to the inner phases of these larger hosts in molecular models. The  $\Delta\delta$  values for the four different kinds of protons in 4-MeOC<sub>6</sub>H<sub>4</sub>Me in its four complexes are very close to one another: for H<sup>a</sup>, with (CH<sub>2</sub>)<sub>4</sub> as a fourth bridge, 4.13; (CH<sub>2</sub>)<sub>5</sub>, 4.06; 1,3-(CH<sub>2</sub>)<sub>2</sub>C<sub>6</sub>H<sub>4</sub>, 4.04; 2,6-(CH<sub>2</sub>)<sub>2</sub>pyridine, 4.07 ppm. The respective  $\Delta\delta$  values for H<sup>b</sup>, H<sup>c</sup>, and H<sup>d</sup> in the four complexes are the following: 0.94, 0.97, 0.94, and 1.03; 1.22, 1.14, 1.08, and 1.19; 4.40, 4.27, 4.25, and 4.27 ppm.

Both model examination and  $\Delta\delta$  values for the H<sup>b</sup> methyl protons of 2-HOC<sub>6</sub>H<sub>4</sub>Me indicate the Me group occupies one of the polar regions of the host in the two complexes prepared and examined. The  $\Delta\delta$  values are as follows: unique bridge (CH<sub>2</sub>)<sub>4</sub>, 4.06; (CH<sub>2</sub>)<sub>5</sub>, 3.99 ppm. The phenolic hydroxyl protons (H<sup>a</sup>) are actually deshielded, with  $\Delta\delta$  values of -0.46 and -0.76, respectively. These acidic protons probably hydrogen bond the oxygens that terminate the bridges at that end of the host in each complex whose hemispheres are occupied by the Me groups. As expected, the H<sup>c</sup> aryl protons *para* to the anchoring Me groups of the guests provide high  $\Delta\delta$  values of 4.09 for the (CH<sub>2</sub>)<sub>4</sub> bridged and 3.92 for the (CH<sub>2</sub>)<sub>5</sub> bridged complexes, respectively. The remaining aryl protons with observable  $\delta$ , H<sup>d</sup> and H<sup>e</sup>, in the two complexes have  $\Delta\delta$  values between 0.78 and 1.45 ppm.

The most crowded complex prepared is **10**⊙1,2,3-(MeO)<sub>3</sub>C<sub>6</sub>H<sub>3</sub>, whose unique bridge is 1,3-(CH<sub>2</sub>)<sub>2</sub>C<sub>6</sub>H<sub>4</sub>. Models of this complex resemble those of **10**⊙1,3-(MeO)<sub>2</sub>C<sub>6</sub>H<sub>4</sub>. The aryl plane of this guest is tilted with respect to the equatorial plane of the host, with one H<sup>a</sup> methyl protruding into one polar region of the host, and the second H<sup>a</sup> methyl protruding into the other polar region. In models of **10**⊙1,2,3-(MeO)<sub>3</sub>C<sub>6</sub>H<sub>3</sub>, the middle MeO group is close to being coplanar with its attached aryl group, which places the H<sup>b</sup> methyl protons in the low-shielding equatorial region. The  $\Delta\delta$  values are consistent with such a structure, being 4.26 for H<sup>a</sup> and 0.81 for H<sup>b</sup> in **10**⊙1,2,3-(MeO)<sub>3</sub>C<sub>6</sub>H<sub>3</sub>, the former being comparable to 4.33 ppm for H<sup>a</sup> in **10**⊙1,3-(MeO)<sub>2</sub>C<sub>6</sub>H<sub>4</sub>.

Important conclusions emerge from these correlations between models of host-guest complexes, and the  $\Delta\delta$  shielding-deshielding patterns of incarcerated guests. (1) When only a single CPK model of a complex can be assembled in which the various parts of each complexing partner are pretty well fixed with respect to one another, the correlation between structural conclusions based on <sup>1</sup>H NMR  $\Delta\delta$  values and the model structure is high. Examples involve complexes of DMA, 1,4-(Me)<sub>2</sub>C<sub>6</sub>H<sub>4</sub>, 1,4-(MeO)<sub>2</sub>C<sub>6</sub>H<sub>4</sub>, 1,2,3-(MeO)<sub>3</sub>C<sub>6</sub>H<sub>3</sub>, and 4-MeOC<sub>6</sub>H<sub>4</sub>Me. (2) When several models of a given host complex can be assembled, the <sup>1</sup>H NMR spectral peaks become broader, and the structural information contained in  $\Delta\delta$  values becomes more restricted and ambiguous. Examples are complexes of 1,2-(MeO)<sub>2</sub>C<sub>6</sub>H<sub>4</sub> and Me<sub>2</sub>SO.

**Representative Examples of Effects on Host NMR Spectra as Lengths and Character of One Bridge of 7 and Its Guests are Changed.** Figure 1 records the interesting parts of the 500 MHz  $^1\text{H}$  NMR spectra in  $\text{CDCl}_3$  at 25  $^\circ\text{C}$  of the host parts of complexes involving **4–6** and **9**. Replacement of one  $\text{O}(\text{CH}_2)_4\text{O}$  bridge in **7** by one  $\text{O–A–O}$  bridge in **4–6** and **9** destroys the formal  $\text{C}_4$  axis of **7**, but leaves a formal mirror plane defined by the two oxygens that terminate the unique bridge, and the two oxygens that terminate the most remote  $\text{O}(\text{CH}_2)_4\text{O}$  bridge. This leads in principle to three different kinds of *interhemispheric*  $\text{OCH}_2$  protons, four different kinds of *intrahemispheric*  $\text{OCH}_2$  protons, and two different methine  $\text{C}_3\text{CH}$  protons.

Some of these closely related protons provide resolved signals in the spectra of Figure 1. For example, in the spectrum of **4**⊙NMP, the three different  $\text{H}^e$  signals for  $\text{OCH}_2^e\text{CH}_2\text{CH}_2\text{CH}_2^e\text{O}$  are close together, whereas in **4**⊙1,4-(Me) $_2\text{C}_6\text{H}_4$ , they are widely separated, probably because of their varying locations with respect to the shielding magnetic fields of their tightly-held aryl guest. In contrast, two sets of  $\text{H}^b$  and  $\text{H}^d$  signals are visible in the **4**⊙NMP spectrum but only one set ( $\text{H}^b$  and  $\text{H}^d$ ) in that of **4**⊙1,4-(Me) $_2\text{C}_6\text{H}_4$ . In the spectrum of **5**⊙NMP, two  $\text{H}^e$ , two  $\text{H}^d$ , but only one  $\text{H}^b$  signals are visible. In the spectrum of **6**⊙NMP, one  $\text{H}^e$ , one  $\text{H}^b$ , and two  $\text{H}^d$  peaks are apparent. In all of these four spectra only one methine signal is observed, but in those of **9**⊙NMP and **9**⊙1,4-(MeO) $_2\text{C}_6\text{H}_4$ , two are clearly discernible. The spectrum of **9**⊙NMP contains a single  $\text{H}^b$ , two  $\text{H}^d$  signals, but only one  $\text{H}^e$  peak. In contrast, that of **9**⊙1,4-(MeO) $_2\text{C}_6\text{H}_4$  provides all three  $\text{H}^e$ , two  $\text{H}^b$ , and two  $\text{H}^d$  signals. These examples as well as many others found in the Experimental Section show how extensively the  $^1\text{H}$  NMR spectra of the host protons vary with guest character.

**Force Field Calculations of Structural Models for 4⊙NMP–7⊙NMP Complexes.** The conformations of hosts and complexes were explored with force field calculations using AMBER\* in the program MACRO-MODEL.<sup>9</sup> This force field has proven useful for the investigation of hemicarceplex conformations and the dynamic processes involved in complexation and decomplexation.<sup>10–12</sup> For computational simplification, the eight  $\text{CH}_2\text{CH}_2\text{C}_6\text{H}_5$  groups of **4–7** were replaced with  $\text{CH}_3$  groups to provide **4-Me**, **5-Me**, **6-Me**, and **7-Me**, respectively. Conformations of the four interhemispheric bridges of **4-Me** to **7-Me** were explored with a Monte Carlo (MC) search by varying the torsional angles. Host **7-Me** was constructed by the graphical input module in MACRO-MODEL. The starting geometries for **6-Me**, **5-Me**, and **4-Me** were obtained by removing one, two, and three methylenes, respectively, from one of the interhemispheric bridges of **7-Me**, and then optimizing the resulting structures with the AMBER\* force field. The total number of MC steps used for each structure was 500, and each MC step began with the geometry of the least-used structure of the previous MC steps. Many low-energy conformers of **7-Me** were located. The conformation of **7-Me** derived from the crystal structure of **7**⊙1,4-

(9) Mohamadi, F.; Richards, N. G. J.; Guida, W. C.; Liskamp, R.; Caufield, C.; Chang, G.; Hendrikson, T.; Still, W. C. *J. Comput. Chem.* **1990**, *11*, 440.

(10) Sheu, C.; Houk, K. N. *J. Am. Chem. Soc.* **1996**, *118*, 8056–8070.

(11) Nakamura, K.; Houk, K. N. *J. Am. Chem. Soc.* **1995**, *117*, 1853–1854.

(12) Houk, K. N.; Nakamura, K.; Sheu, C.; Keating, A. E. *Science* **1996**, *273*, 627–629.

host proton labels:

$\text{H}^a$ ,  $\text{OCH}_2^a\text{O}$ ,  $\text{OCH}_2^a\text{CH}_2^a\text{O}$  or  $\text{OCH}_2^a\text{CH}_2\text{CH}_2^a\text{O}$

$\text{H}^b$ , outer proton of  $\text{OCH}_2^b\text{O}$ , intrahemispheric

$\text{H}^c$ , methine

$\text{H}^d$ , inner proton of  $\text{OCH}_2^d\text{O}$ , intrahemispheric

$\text{H}^e$ ,  $\text{OCH}_2^e\text{CH}_2\text{CH}_2\text{CH}_2^e\text{O}$

$\text{H}^f$ , guest H

$\text{H}^g$ ,  $(\text{CH}_2^g)_2$ quinoxaline of **9**

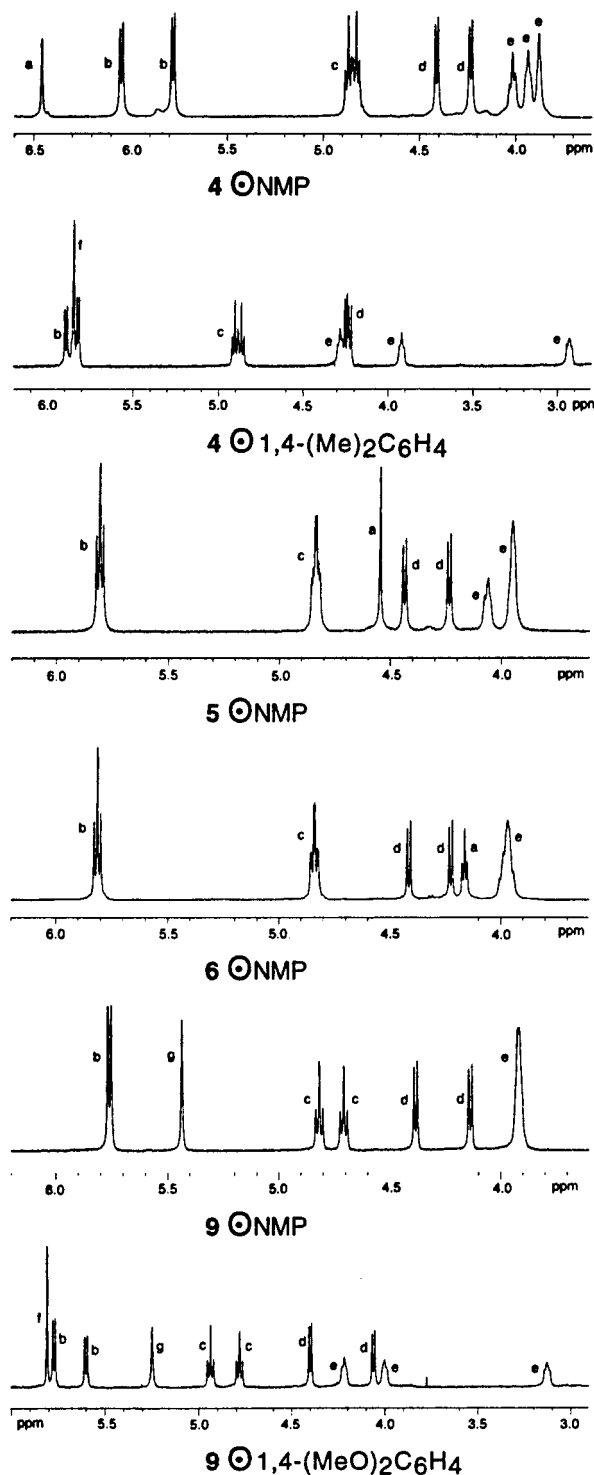


**Figure 1.** Partial 500 MHz  $^1\text{H}$  NMR spectra of hosts of **4**⊙Guest, **5**⊙Guest, **6**⊙Guest, and **9**⊙Guest.

$\text{Me}_2\text{C}_6\text{H}_4$ <sup>6</sup> is very close structurally to the global minimum obtained by the MC search, and its energy is only 0.6



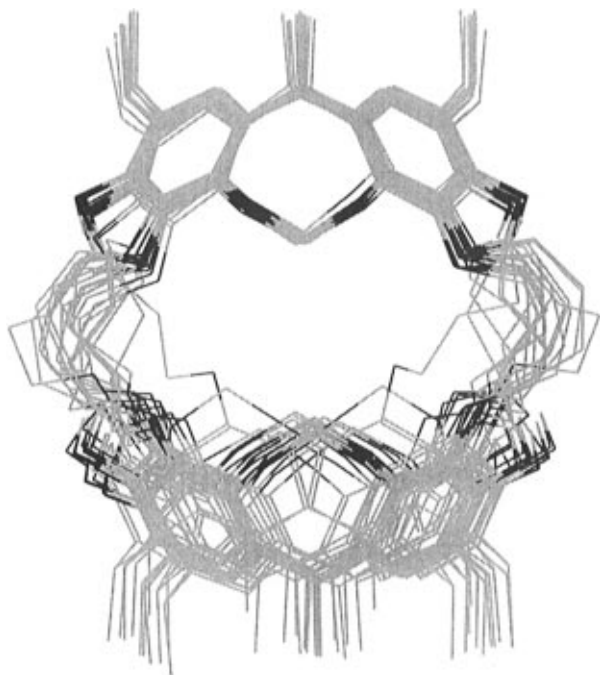


**Figure 2.** Superposition of 10 low-energy conformers of **7-Me**.

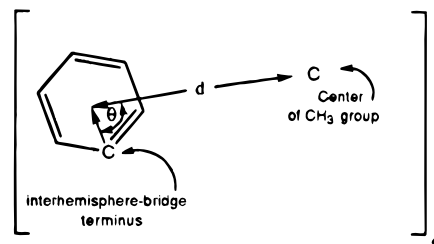
kcal mol<sup>-1</sup> higher by AMBER\*. The northern and southern bowls of the hemicarcerand are very rigid and the flexibility of the molecule is mainly due to the interhemispheric bridges. Figure 2 is the superposition of 10 low-energy conformers, all of which are within 1.5 kcal mol<sup>-1</sup> of the global minimum.

Starting geometries for the NMP complexes were obtained manually by docking the NMP guest inside the cavity of the hemicarcerand in various orientations. These were energy-minimized with the AMBER\* force field. The lowest-energy conformer of each carceplex was then used as the starting geometry in an optimization utilizing the simulated annealing method. The cooling process was linear and continuous from 500 K to 50 K over a 1000 ps molecular dynamics simulation. The structure of the lowest-energy conformer for each complex is found in Figure 3.

The best plane of the guest in the calculated structures of Figure 3 is roughly placed in the plane of the page, with the *N*-methyl pointing upward into the north polar cap. In all four structures, the best plane of the guest and page roughly bisects two of the portals, with two of the bridges flanking the C=O group, and two bridges flanking the two H's of the NCH<sub>2</sub> group. The four CH<sub>2</sub>CH<sub>2</sub>CH<sub>2</sub>N hydrogens of the guest point generally toward the southern polar part of the host, which is consistent with the substantial upfield shifts in their <sup>1</sup>H NMR spectra.

A general and important feature of these calculated structures is that the electron pairs of the oxygen termini of the *interhemispheric bridges* all face inward, opposite to the directions in which the *intrahemispheric spanner* oxygens face, thus minimizing the energy of their dipole-dipole interactions. Consequently, the carbon chains of the interhemispheric bridges lie outside of the distorted cube defined by the eight oxygens to which these chains are attached. In these respects the calculated structure of host **7** in **7-Me**⊙NMP resembles the crystal structures of **7**⊙**Guests**, many of which have been determined,<sup>6</sup> and also the structures of **8**⊙4-MeC<sub>6</sub>H<sub>4</sub>OMe and **10**⊙CHCl<sub>3</sub> reported here (Chart 3).

Analysis of the calculated structures of **4-Me** to **7-Me** provides the average distance between two planes, each defined by the four aryl carbons at the termini of the four interhemispheric bridges in the respective northern and southern hemispheres. Table 2 lists the results. These distances (Å) increase monotonically with increasing lengths of the unique bridges in the hosts and range from 5.1 to 6.0 Å. Two other parameters locate the center of the guest NMP methyl group with respect to the center of the four proximate benzenes of the host: the distance (*d*) between these two centers: the average deviation from 90° of the angle  $\theta$  between vector **d** and one connecting the center of the benzene with the terminus of the interhemispheric bridge. These parameters are visualized in diagram 1.



These distances and  $\theta$  angle deviations are listed in Table 2, and they correlate, respectively, with the number of methylenes in the unique bridges as follows: CH<sub>2</sub>, 3.5 Å and 9.8°; (CH<sub>2</sub>)<sub>2</sub>, 3.8 Å and 4.9°; (CH<sub>2</sub>)<sub>3</sub>, 4.0 Å and 4.5°; (CH<sub>2</sub>)<sub>4</sub>, 3.9 Å and 4.4°. These parameters also correlate with the upfield chemical shift changes in the <sup>1</sup>H NMR spectral  $\Delta\delta$  values for the methyl group of NMP upon incarceration in **4**–**7**, listed in Table 2.

**Approximate Half-Lives for Decomplexation of Complexes Involving Largest Hosts and Guests.** Much qualitative information dealing with complexes stable or unstable to isolation conditions is found in Chart 1. Isolation involved evaporation of aprotic dipolar solvents under vacuum under 45 °C, flooding the reaction mixtures with methanol, and subjecting the methanol-washed precipitate to thick layer chromatography with CHCl<sub>3</sub> as the mobile phase. Complexes of **4**, **5**, **6**, **7**,<sup>6</sup> and **9** with NMP, DMSO, and DMA as guests are stable to these manipulations, whereas free **6** and **7** did not complex under similar conditions (Chart 1). In contrast, **8**⊙NMP, **10**⊙NMP, and **11**⊙NMP went to **8**⊙CHCl<sub>3</sub>, **10**⊙CHCl<sub>3</sub> and **11**⊙CHCl<sub>3</sub> under the same conditions. Complexation of **4**–**7** or **9** and decomplexation of their complexes involves guests passing through 23- to 26-membered rings. Only guests as small as CH<sub>2</sub>Cl<sub>2</sub> or pentane (but not CHCl<sub>3</sub>) readily entered and departed the interior of **7** in solution at 25 °C.<sup>6</sup> However, CHCl<sub>3</sub> readily passed through the 27-membered ring portals of **8**, **10**, and **11**. Temperatures of 100–200 °C appear needed for hosts with 26-membered and 27-membered ring portals to complex or decomplex guests containing 6–12 atoms other than hydrogen (Chart 2 and prior work<sup>3,6</sup>).

Because little was known about the kinetic stability of complexes of hosts with 27-membered ring portals, we determined the approximate half-lives for decomplexation in CDCl<sub>3</sub> at 25 °C of the complexes between **7**, **8**, **10** and 4-MeC<sub>6</sub>H<sub>4</sub>OMe, 4-MeOC<sub>6</sub>H<sub>4</sub>OMe, and 3-MeOC<sub>6</sub>H<sub>4</sub>OMe. Table 3 records the *t*<sub>1/2</sub> values for those decomplexations that could be detected.

Complexes of **7** with all three guests gave no <sup>1</sup>H NMR-detectable uncomplexed guest after 336–720 h. Half-

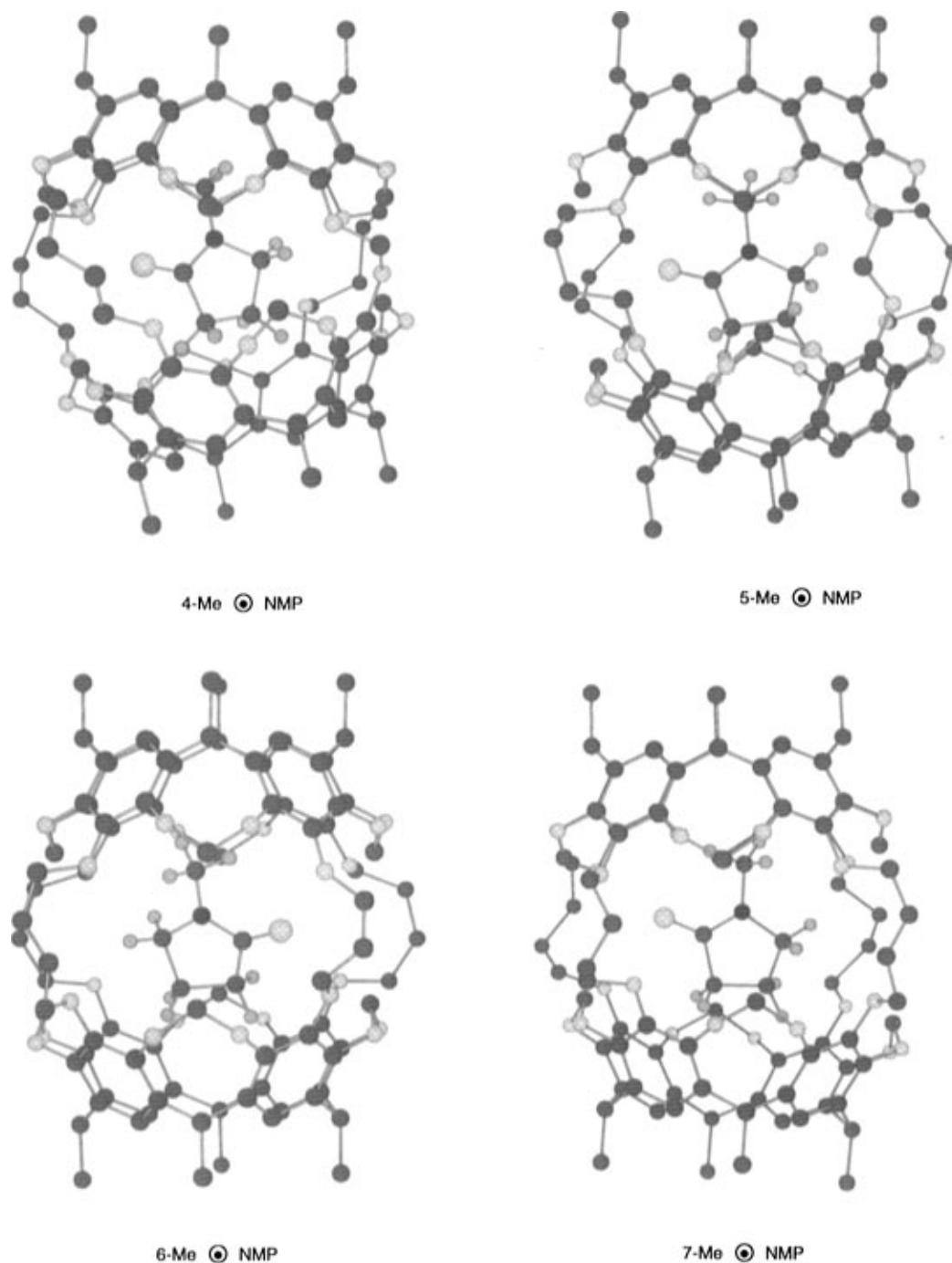


**Figure 3.** Force field calculated structures derived for molecules of **4**⊙NMP, **5**⊙NMP, **6**⊙NMP, and **7**⊙NMP, simplified by substitution of CH<sub>3</sub> for CH<sub>2</sub>CH<sub>2</sub>C<sub>6</sub>H<sub>5</sub> groups in the hosts to give, respectively, **4-Me**⊙NMP, **5-Me**⊙NMP, **6-Me**⊙NMP, and **7-Me**⊙NMP. In the drawings, H atoms are omitted from the hosts and the unique bridges are on the right, toward the viewer.

**Table 2.** Results of Force Field Calculations of Structures of NMP Complexes of Hosts **4-Me-7-Me**<sup>a</sup>

complex modeled	unique bridge	average distances between centers (Å)		average deviation of ⊙ from 90 ° <sup>c</sup>	observed <sup>1</sup> H NMR Δδ for guest CH <sub>3</sub> (ppm) <sup>d</sup>
		interhemispheric bridge termini <sup>b</sup>	NMP methyl to aryl faces <sup>c</sup>		
<b>4-Me</b> ⊙NMP	OCH <sub>2</sub> O	5.1	3.5	9.8	3.83
<b>5-Me</b> ⊙NMP	O(CH <sub>2</sub> ) <sub>2</sub> O	5.7	3.8	4.9	3.63
<b>6-Me</b> ⊙NMP	O(CH <sub>2</sub> ) <sub>3</sub> O	5.9	4.0	4.5	3.60
<b>7-Me</b> ⊙NMP	O(CH <sub>2</sub> ) <sub>4</sub> O	6.0	3.9	4.4	3.59

<sup>a</sup> The eight CH<sub>2</sub>CH<sub>2</sub>C<sub>6</sub>H<sub>5</sub> feet of hosts **4-7** have been replaced by CH<sub>3</sub> feet to simplify the calculations. <sup>b</sup> Hemispheric planes defined by aryl carbon termini of bridges. <sup>c</sup> See Diagram 1. <sup>d</sup> H<sup>a</sup> protons' Δδ values, Table 1.

life values for decomplexations of **8**⊙4-MeC<sub>6</sub>H<sub>4</sub>OMe, **8**⊙3-MeOC<sub>6</sub>H<sub>4</sub>OMe, and **8**⊙4-MeOC<sub>6</sub>H<sub>4</sub>OMe are as follows: >720 h, >600 h, and 310 h. Half-life values for decomplexations of **10**⊙3-MeOC<sub>6</sub>H<sub>4</sub>OMe, **10**⊙4-MeC<sub>6</sub>H<sub>4</sub>OMe,

and **10**⊙4-MeOC<sub>6</sub>H<sub>4</sub>OMe decreased respectively as follows: 250 h, 85 h, and 8 h.

These results emphasize how large a difference one methylene can make in a portal's ability to allow or

**Table 3. Decomplexation Half-Lives in Hours in CDCl<sub>3</sub> at 25 °C**

guest structure	no.	host		t <sub>1/2</sub> (h)
		unique bridge	largest ring (portal)	
	7	O(CH <sub>2</sub> ) <sub>4</sub> O	26-membered	>> 720 <sup>a</sup>
	8	O(CH <sub>2</sub> ) <sub>5</sub> O	27-membered	>720 <sup>b</sup>
	10	1,3-O(CH <sub>2</sub> ) <sub>2</sub> C <sub>6</sub> H <sub>4</sub>	27-membered	85
	7	O(CH <sub>2</sub> ) <sub>4</sub> O	26-membered	>> 336 <sup>a</sup>
	8	O(CH <sub>2</sub> ) <sub>5</sub> O	27-membered	310
	10	1,3-O(CH <sub>2</sub> ) <sub>2</sub> C <sub>6</sub> H <sub>4</sub>	27-membered	8
	7	O(CH <sub>2</sub> ) <sub>4</sub> O	26-membered	>> 720 <sup>a</sup>
	8	O(CH <sub>2</sub> ) <sub>5</sub> O	27-membered	>600 <sup>b</sup>
	10	1,3-(OCH <sub>2</sub> ) <sub>2</sub> C <sub>6</sub> H <sub>4</sub>	27-membered	250

<sup>a</sup> No decomplexation detected after this time. <sup>b</sup> Less than 10% decomplexation after this time.

disallow passage of a guest from the inner to the bulk phase of a host at 25 °C. Thus 7⊙guest<sup>6</sup> and 12⊙guest<sup>14</sup> complexes containing 26-membered ring portals are stable indefinitely at 25 °C in solvent (such as CDCl<sub>2</sub>-CDCl<sub>2</sub>) with guests as small as CH<sub>3</sub>CH<sub>2</sub>I, CH<sub>3</sub>COCH<sub>3</sub>, (CH<sub>2</sub>)<sub>4</sub>O, and CH<sub>3</sub>CO<sub>2</sub>CH<sub>2</sub>CH<sub>3</sub>,<sup>3,6</sup> as well as larger guests such as 4-MeC<sub>6</sub>H<sub>4</sub>OMe, 3-MeOC<sub>6</sub>H<sub>4</sub>OMe, and 4-MeOC<sub>6</sub>H<sub>4</sub>-OMe in CDCl<sub>3</sub>. Host 8⊙guest with two 27-membered ring portals has decomplexation half-lives in the hundreds of hours, and 10⊙guest with two 27-membered ring portals with a *m*-xylyl group substituted for a (CH<sub>2</sub>)<sub>3</sub> moiety in the middle of the unique bridge has half lives that range from 250 to 8 h for the three disubstituted benzene guests. Thus the *m*-xylyl group offers somewhat less resistance to guest passage than the (CH<sub>2</sub>)<sub>3</sub> group, probably because of the latter's six hydrogens.

**Force Field Calculations of Binding Energies and Activation Energies for Decomplexation of 7-Me⊙NMP, 8-Me⊙NMP, and 10-Me⊙NMP.** To obtain further insight regarding the differences in stabilities of complexes 7⊙NMP, 8⊙NMP, and 10⊙NMP, binding energies in the gas phase and in chloroform were calculated using the AMBER\* force field program mentioned previously. As before, the calculations were simplified by replacing the eight CH<sub>2</sub>CH<sub>2</sub>C<sub>6</sub>H<sub>5</sub> groups of each host with eight CH<sub>3</sub> groups to give, respectively, 7-Me⊙NMP, 8-Me⊙NMP, and 10-Me⊙NMP. The binding energies are defined by the expression

$$\Delta E = E_{(\text{complex})} - [E_{(\text{host})} + E_{(\text{guest})}]$$

and are listed in Table 4 for both the gas phase and in CHCl<sub>3</sub> solution (with GB/SA<sup>5</sup> chloroform treatment).

Gas phase calculations were also performed to estimate the activation energies for guest escape following a procedure described earlier.<sup>10,11</sup> A reaction coordinate,  $\lambda$ , was defined along which the guest was forced to pass through the larger of the equatorial portals.<sup>11</sup> As illustrated in Figure 4, the dotted lines connect a dummy atom (Du) with the four aryl carbon atoms 20 Å distant attached to the two interhemispheric bridges that define

**Table 4. Force Field AMBER\* Calculations of Binding Energies and Activation Energies for Decomplexation of 7-Me⊙NMP, 8-Me⊙NMP, and 10-Me⊙NMP, and the Dissection of the Activation Energies for Decomplexation into Intrinsic and Constrictive Components**

phase	energies (kcal mol <sup>-1</sup> )	complex		
		7-Me⊙NMP	8-Me⊙NMP	10-Me⊙NMP
gas	$\Delta E$	-19.3	-19.8	-18.3
CHCl <sub>3</sub>	$\Delta E$	-11.5	-13.4	-12.2
gas	$\Delta E^\ddagger_{(\text{decomplex})}$	39.0	27.1	21.3
gas	$\Delta E^\ddagger_{(\text{intrinsic})}$	19.3	19.8	18.3
gas	$\Delta E^\ddagger_{(\text{constrictive})}$	19.7	7.3	3.0

one of the larger portals. The reaction coordinate connects Du with the center of the methyl of incarcerated NMP. By gradually decreasing the distance between the guest molecule and the defined dummy atom, the activation energy for the guest escape process was estimated by energy minimization for each step. For the host molecules with all their intrahemispheric bridges (spanners) in their favored chair conformations, the activation energy barriers for the decomplexation of NMP from model hosts 7-Me, 8-Me, and 10-Me were calculated. Figure 5 is a plot of energy versus distance for the three complexes from which the  $\Delta E^\ddagger_{(\text{decomplex})}$  values were taken.

The absolute values listed (Table 4) of 39.0, 27.1, and 21.3 kcal mol<sup>-1</sup> are probably somewhat high, but their relative values are meaningful. Particularly interesting is the dissection of these activation energies into intrinsic and constrictive components, using the equation,

$$\Delta E^\ddagger_{(\text{constrictive})} = \Delta E^\ddagger_{(\text{decomplex})} - (-\Delta E) = \Delta E^\ddagger_{(\text{complexation})}^{14}$$

Table 4 lists the  $\Delta E^\ddagger_{(\text{constrictive})}$  values, which are as follows: for 7-Me⊙NMP, 19.7; for 8-Me⊙NMP, 7.3; for 10-Me⊙NMP, 3.0 kcal mol<sup>-1</sup>. The percent contribution made by constrictive binding to the total activation energy for the three respective decomplexations is 51%, 27%, and 14%.

The thermodynamic  $\Delta E$  values found in Table 4 correlate well with expectations based on molecular model examinations.

The  $\Delta E$  values for the calculated binding energies for 7-Me⊙NMP, 8-Me⊙NMP, and 10-Me⊙NMP in the gas phase provide an average of 19.1 ± 0.8 kcal mol<sup>-1</sup>, and in CHCl<sub>3</sub>, an average of 12.4 ± 1.0 kcal mol<sup>-1</sup>. The maximum spread in each set of three values is only 2 kcal mol<sup>-1</sup>, which correlates with the facts that the NMP guest is common to the three complexes, the three hosts differ only in one of their bridges, and these unique bridges differ mainly in their lengths and in the small differences in numbers of stabilizing host-guest contacts available in these hosts.

The gas phase transition state energies for complexation-decomplexation differ dramatically, that for 7-Me⊙NMP being ≈ 12 kcal mol<sup>-1</sup> higher than that for 8-Me⊙NMP, which in turn is 5.8 kcal mol<sup>-1</sup> higher than that for 10-Me⊙NMP. This order correlates with the order listed in Table 3 for the *t*<sub>1/2</sub> values for the decomplexations of the same hosts as follows: 7⊙guests > 8⊙guests > 10⊙guests. Thus the differences between the kinetic stabilities of the three hemiarcerplexes are much greater than the differences in thermodynamic stabilities.

Striking features of the energy-distance profile for decomplexation of the three model hosts shown in Figure

(13) Still, W. C.; Tempczyk, A.; Hawley, R. C.; Hendrickson, T. J. *Am. Chem. Soc.* **1990**, *112*, 6127-6129.

(14) Cram, D. J.; Blanda, M. T.; Paek, K.; Knobler, C. B. *J. Am. Chem. Soc.* **1992**, *114*, 7765-7773.

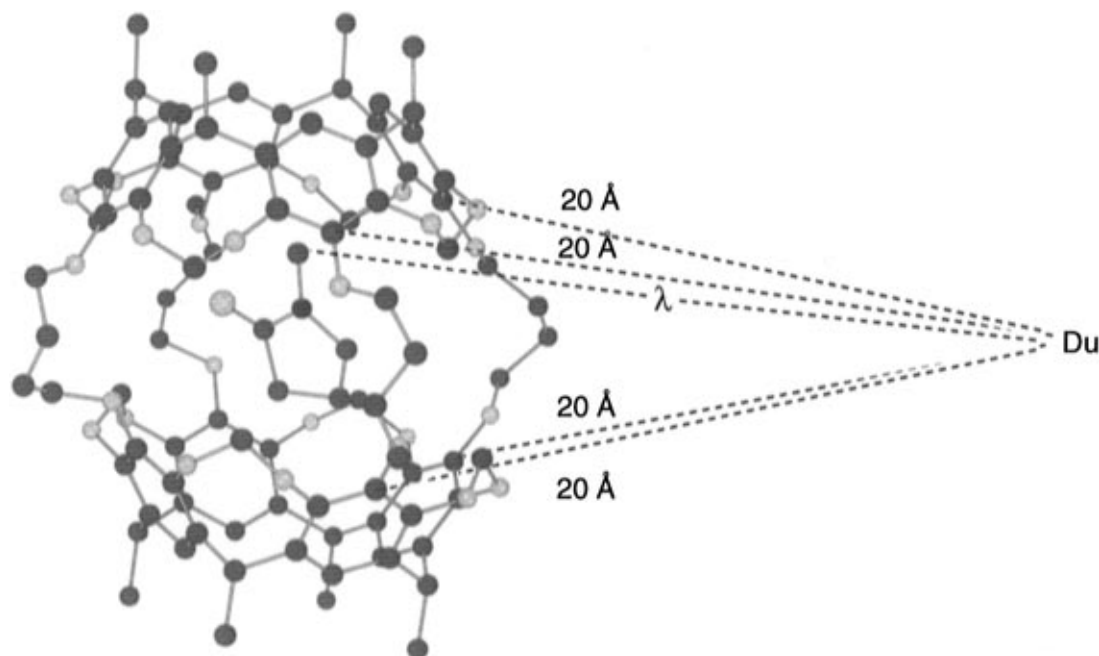


**Figure 4.** Definition of reaction coordinate  $\lambda$  for activation energy calculations. See text.

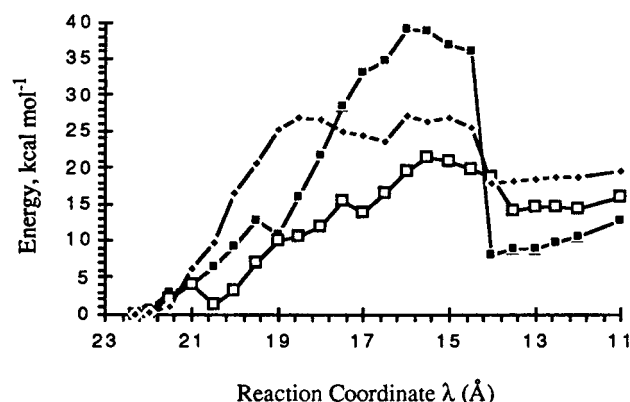


**Figure 5.** Energy profile for the decomplexation of the NMP guest in vacuum. ■: **7-Me⊙NMP**; ◆: **8-Me⊙NMP**; □: **10-Me⊙NMP**.

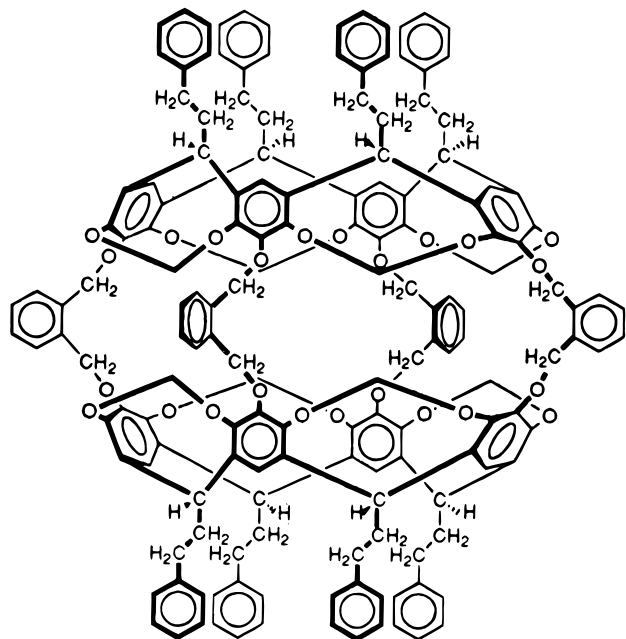
5 are as follows: (1) the energy falls very abruptly at a distance of about 14 Å, particularly for **7-Me⊙NMP**; (2) the curves contain some fine structure and several maxima; (3) the energy peaks spread over 5–6 Å for all three complexes. All three features correlate with what is suggested by the mechanical force and deformations needed to separate host from guest in CPK models of these complexes. Large numbers of bond angles must be adjusted, particularly in the host, to synchronize with guest rotations and with guest penetrations and expansions of the portals. The distance the guest must travel before it is free of the expanded portal in CPK models is in the 5–7 Å range. Even multiple mechanical barriers are encountered in these model separations.

Although hosts with longer fourth bridges ((CH<sub>2</sub>)<sub>5</sub> and 1,3-(CH<sub>2</sub>)<sub>2</sub>C<sub>6</sub>H<sub>4</sub>) than (CH<sub>2</sub>)<sub>4</sub> do not have significantly greater inner volumes (as seen in Table 4, the stabilization energies for **7-Me⊙NMP**, **8-Me⊙NMP**, and **10-Me⊙NMP** are very similar), the two portals that flank the longer fourth bridges dramatically increase in size and conformational adaptivity for guest passages. The portal effect can be seen in Figure 5, where the energy peak for **7-Me⊙NMP** (26-membered ring portals) is somewhat sharper and narrower than the peaks for 27-

membered ring portals (**8-Me⊙NMP**, **10-Me⊙NMP**), which spread over 6–7 Å. In earlier studies,<sup>10–12</sup> we proposed an alternative mechanism involving the interconversions of the intrahemispheric spanners of hemicarcerands from chairlike to boatlike conformations to explain the escape pathway of acetonitrile molecules from the tetrasulfide hemicarceplex.<sup>11</sup> This gating phenomenon also plays an important role in obtaining stable complexes.<sup>12</sup> The conversion of the intrahemispheric spanners from low-energy chairlike to higher-energy boatlike conformations enlarges the portals and reduces the steric repulsion between host and guest. This is especially true when the interhemispheric bridges are short (for example, 20-membered ring portals). When the interhemispheric bridges are longer, the methylene gate plays a less important role. The size and shape of the guest molecule also affect the importance of the gating mechanism. In the present case, the steric repulsive energy reduced by the gating process is approximately equal to the energy cost for the host to adopt the higher-energy conformation.

The greatest weaknesses of the activation energy calculations are the omissions of solvent and entropy. In an earlier study, the decomplexation rate for **12⊙DMA**<sup>14</sup> was found to vary by a factor of about 50 as solvent was changed from C<sub>6</sub>D<sub>5</sub>Br to C<sub>6</sub>D<sub>5</sub>CD<sub>3</sub>. Free energies, enthalpies, and entropies of activation for decomplexation of **12⊙DMA**, **12⊙MeCO<sub>2</sub>CH<sub>2</sub>Me**, **12⊙MeCOCH<sub>2</sub>Me**, and **12⊙MeC<sub>6</sub>H<sub>5</sub>** in 1,2-(CD<sub>3</sub>)<sub>2</sub>C<sub>6</sub>D<sub>4</sub> were measured at 100 °C. The contributions of  $\Delta S^\ddagger$  to the  $\Delta G^\ddagger$  for the four complexes varied from 25 to 51%. The contribution of constrictive binding to the free energies of activation for decomplexations of the four complexes varied from 82 to 88%. Host **12** has four 26-membered ring portals as does **7**, but each OCH<sub>2</sub>C<sub>6</sub>H<sub>4</sub>CH<sub>2</sub>O bridge in **12** is conformationally less adaptive than each O(CH<sub>2</sub>)<sub>4</sub>O bridge in **7**. Clearly, much exploration of decomplexation phenomena remains to be done.

**Summary.** Seven new carcerand or hemicarcerand systems have been synthesized, all of which contain two rigid bowls connected by three O(CH<sub>2</sub>)<sub>4</sub>O bridges put in



12

place by a shell closure. In a separate step, a fourth unique bridge was introduced by sealing into the host's inner phase appropriately sized guests in the medium. Three of the unique bridges are shorter ( $\text{O}(\text{CH}_2)_2\text{O}$ ,  $\text{O}(\text{CH}_2)_2\text{O}$ , and  $\text{O}(\text{CH}_2)_3\text{O}$ ), one is about the same length (2,3- $(\text{OCH}_2)_2$ quinoxaline), and three are longer ( $\text{O}(\text{CH}_2)_5\text{O}$ , 1,3- $(\text{OCH}_2)_2\text{C}_6\text{H}_4$ , and 2,6- $(\text{OCH}_2)_2$ pyridine) than the other three bridges. Thirty-six new hemicarceplexes, involving thirteen different guests, were prepared either by sealing in or by thermally-induced guest exchange driven by mass law. They were characterized, and their  $^1\text{H}$  NMR spectral changes were correlated with changes in the fourth bridge. The crystal structures of two complexes were determined and compared with expectations based on molecular model examinations. Force field AMBER\* calculations were made of the structures of four NMP complexes containing homologically related unique bridges ( $\text{O}(\text{CH}_2)_n\text{O}$ ,  $n = 1-4$ ) and were similar to those based on crystal structures of similar hemicarceplexes. Half-lives for decomplexations of hemicarceplexes involving three of the largest hosts and guests were correlated with portal macroring sizes. Decomplexations were modeled with AMBER\* force field calculations and the results found to qualitatively correlate with experimental facts.

### Experimental Section

**General.** All chemicals were reagent grade and used directly unless otherwise noted. Dimethylacetamide (DMA), *N*-methylpyrrolidinone (NMP), and dimethyl sulfoxide (DMSO) were stored over (24 h heated at 320 °C) 3-Å molecular sieves and degassed under high vacuum just before use. A 360-MHz spectrometer was used to record  $^1\text{H}$  NMR spectra unless otherwise noted. Spectra taken in  $\text{CDCl}_3$  were referenced to residual  $\text{CHCl}_3$  at 7.26 ppm. FAB MS were determined on a ZAB SE instrument with 3-nitrobenzyl alcohol (NOBA) as a matrix and Xe as carrier gas. Gravity chromatography was performed on silica gel 60 (70–230 mesh). Thin-layer chromatography involved glass-backed plates (silica gel 60,  $F_{245}$ , 0.25 mm).

**8,9,10,11,39,40,41,42-Octahydro-1,18,26,28,53,55,63,74-octaphenethyl-34,47-(epoxybutanoxy)-20,24:57,61-dimethano-2,5:2:3,51:16,30:17,29-tetrametheno-1*H*,18*H*,26*H*,**

**28*H*,53*H*,55*H*-bis[1,3]benzodioxocino[9,8-*d'*9',8'-*d*]bis[1,3]benzodioxocino[9',10':17,18;10'',9'':25,26][1,3,6,11,14,16,19,24]octaoxacyclohexacosino[4,5-*f*:13,12-*j*]bis[1,3]benzodioxol, Stereoisomer 2.** Into a 1 L one-neck round-bottom flask equipped with a magnetic stirrer and blanketed with argon were placed 1 g (1.0 mmol) of **1**, 200 mL of degassed NMP, and 6.5 g of  $\text{Cs}_2\text{CO}_3$ . The reaction mixture was stirred at 25 °C for 1 min after which 0.97 g (4.0 mmol) of 1,4-butanediol dimesylate was added. The mixture was stirred for 16–18 h and then poured into 500 mL of 10% NaCl (aq). After 30 min, the precipitate that formed was filtered and chromatographed with 0.5% EtOAc in  $\text{CH}_2\text{Cl}_2$  followed by 3% EtOAc in  $\text{CH}_2\text{Cl}_2$  to give **2** (30–40%):  $^1\text{H}$  NMR  $\delta$  1.98 (4 H, br s); 2.03 (8 H, br s); 2.48 (16 H, m); 2.68 (16 H, m); 3.88 (4 H, br s); 3.92 (8 H, br s); 4.26 (8 H, overlapping d,  $J = 8.1$  Hz); 4.82 (8 H, m); 5.85 (4 H, d,  $J = 7.0$  Hz); 5.97 (4 H, d,  $J = 6.9$  Hz); 6.21 (2 H, s); 6.64 (2 H, s); 6.82 (4 H, s); 6.85 (2 H, s); 7.16 (16 H, m); 7.23 (24 H, m); FAB MS  $m/e$  (2194.9,  $\text{M}^+$ ), 2197.1 (100). Anal. Calcd for  $\text{C}_{140}\text{H}_{130}\text{O}_{24}\cdot 5\text{H}_2\text{O}$ : C, 73.54; H, 6.17. Found: C, 73.67; H, 6.04.

**8,9,10,11,39,40,41,42-Octahydro-1,18,26,28,53,55,63,77-octaphenethyl-34,47-(epoxybutanoxy)-20,24:57,61-dimethano-2,5:17,29-dimetheno-3,51,16,30-(methoxymethanoxy)metheno-1*H*,18*H*,26*H*,28*H*,53*H*,55*H*-bis[1,3]benzodioxocino[9,8-*d'*9',8'-*d*]bis[1,3]benzodioxocino[9',10':17,18;10'',9'':25,26][1,3,6,11,14,16,19,24]octaoxacyclohexacosino[4,5-*f*:13,12-*j*]bis[1,3]benzodioxol, Stereoisomer 4 $\odot$ NMP.** Diol host **2**<sup>4</sup> (100 mg, 0.045 mmol), 50 mL of NMP, 1 g of pulverized  $\text{Cs}_2\text{CO}_3$ , and 30  $\mu\text{L}$  (0.46 mmol) of  $\text{BrCH}_2\text{Cl}$  were stirred at 65 °C for 24 h, and 30  $\mu\text{L}$  (0.46 mmol) of  $\text{BrCH}_2\text{Cl}$  was added. After stirring at 65 °C for another 24 h, the solvent was removed in vacuo and the residue dissolved in  $\text{CHCl}_3$ . The remaining solids were filtered through a 1 cm pad of Celite, and the solvent was rotary evaporated to ~3 mL volume and poured into 100 mL of methanol. The precipitate that formed was filtered and chromatographed on a preparative TLC plate with  $\text{CHCl}_3$  to give 55 mg (53%) of 4 $\odot$ NMP:  $^1\text{H}$  NMR  $\delta$  -1.25 (2 H, q); -1.13 (3 H, s); -0.90 (2 H, t,  $J = 7.2$  Hz); 1.80 (2 H, t,  $J = 7.0$  Hz); 1.95 (4 H, br s); 1.97 (4 H, br s); 2.17 (4 H, br s); 2.49 (16 H, m); 2.67 (16 H, m); 3.89 (4 H, br s); 3.94 (4 H, t); 4.01 (4 H, t,  $J = 7.1$  Hz); 4.24 (4 H, d,  $J = 7.1$  Hz); 4.42 (4 H, d,  $J = 7.1$  Hz); 4.86 (8 H, m); 5.79 (4 H, d,  $J = 7.3$  Hz); 6.05 (4 H, d,  $J = 7.3$  Hz); 6.46 (2 H, s); 6.84 (6 H, s); 6.89 (2 H, s); 7.15 (16 H, m); 7.23 (24 H, m); FAB MS,  $m/e$  (2306.0,  $\text{M}^+$ ), 2307.0 (100). Anal. Calcd for  $\text{C}_{146}\text{H}_{139}\text{NO}_{25}$ : C, 75.99; H, 6.07. Found: C, 76.23; H, 5.75.

**4 $\odot$ DMSO.** Application of procedure A to 100 mg (0.045 mmol) of diol host **2**, 50 mL of DMSO, 1 g of  $\text{Cs}_2\text{CO}_3$ , and 60  $\mu\text{L}$  (0.92 mmol) of  $\text{BrCH}_2\text{Cl}$  gave 52 mg (51%) of 4 $\odot$ DMSO:  $^1\text{H}$  NMR  $\delta$  -0.68 (6 H, s); 1.95–2.19 (12 H, m); 2.49 (16 H, m); 2.68 (16 H, m); 3.82 (4 H, t,  $J = 7.1$  Hz); 3.91 (4 H, br s); 3.97 (4 H, t,  $J = 7.1$  Hz); 4.13 (4 H, d,  $J = 7.3$  Hz); 4.32 (4 H, d,  $J = 7.3$  Hz); 4.86 (8 H, m); 5.85 (4 H, d,  $J = 7.3$  Hz); 6.09 (4 H, d,  $J = 7.3$  Hz); 6.54 (2 H, s); 6.80 (2 H, s); 6.84 (4 H, s); 6.92 (2 H, s); 7.17 (16 H, m); 7.24 (24 H, m); FAB MS  $m/e$  (2284.9,  $\text{M}^+$ ), 2287.1 (40); 2209 (100). Anal. Calcd for  $\text{C}_{143}\text{H}_{136}\text{O}_{25}\text{S}$ : C, 75.11; H, 5.99. Found: C, 75.36; H, 5.98.

**4 $\odot$ DMA.** Application of procedure A to 100 mg (0.045 mmol) of diol host **2**, 50 mL of DMA, 1 g of  $\text{Cs}_2\text{CO}_3$ , and 60  $\mu\text{L}$  (0.92 mmol) of  $\text{BrCH}_2\text{Cl}$  gave 56 mg of 4 $\odot$ DMA (54%):  $^1\text{H}$  NMR  $\delta$  -1.92 (3 H, s); -0.90 (3 H, s); 1.58 (3 H, s); 1.85–2.22 (12 H, m); 2.49 (16 H, m); 2.68 (16 H, m); 3.82 (4 H, t,  $J = 6.9$  Hz); 3.92 (4 H, br s); 4.00 (4 H, t,  $J = 6.9$  Hz); 4.16 (4 H, d,  $J = 7.2$  Hz); 4.54 (4 H, d,  $J = 7.2$  Hz); 4.85 (8 H, m); 5.81 (4 H, d,  $J = 7.2$  Hz); 6.05 (4 H, d,  $J = 7.2$  Hz); 6.47 (2 H, s); 6.77 (2 H, s); 6.83 (4 H, s); 6.92 (2 H, s); 7.17 (16 H, m); 7.24 (24 H, m); FAB MS  $m/e$  (2294.0,  $\text{M}^+$ ) 2295.3 (30), 2208.3 (100). Anal. Calcd for  $\text{C}_{145}\text{H}_{139}\text{NO}_{25}$ : C, 75.86; H, 6.10. Found: C, 76.09; H, 6.37.

**4 $\odot$ 1,4-Me<sub>2</sub>C<sub>6</sub>H<sub>4</sub>.** Procedure B. Into a Pyrex test tube capped with a rubber septum were placed 30 mg (0.013 mmol) of 4 $\odot$ DMA and 1 mL of *p*-xylene. This mixture was heated at 140 °C for 3 days and poured into 50 mL of methanol. The precipitate that formed was filtered and chromatographed on a preparative TLC plate with  $\text{CHCl}_3$  to give 26 mg (85%) of 4 $\odot$ 1,4-Me<sub>2</sub>C<sub>6</sub>H<sub>4</sub>:  $^1\text{H}$  NMR  $\delta$  -2.02 (6 H, s); 1.09 (4 H, m); 2.08

(4 H, m); 2.17 (4 H, m); 2.52 (16 H, m); 2.69 (16 H, m); 2.93 (4 H, t); 3.92 (4 H, br s); 4.24 (8 H, t,  $J = 7.8$  Hz); 4.27 (4 H, t); 4.89 (8 H, m); 5.82 (4H, d,  $J = 6.9$  Hz); 5.85 (4 H, s); 5.89 (4H, d,  $J = 6.9$  Hz); 6.82 (4 H, s); 6.88 (2 H, s); 6.94 (2 H, s); 7.16 (16 H, m); 7.23 (24 H, m); FAB MS,  $m/e$  (2313.0,  $M^+$ ) 2314.0 (40), 2208.3 (100). Anal. Calcd for  $C_{149}H_{140}O_{24} \cdot 2H_2O$ : C, 76.13; H, 6.17. Found: C, 76.14; H, 5.99.

**8,9,10,11,39,40,41,42-Octahydro-1,18,26,28,53,55,63,78-octaphenethyl-34,47-(epoxybutanoxy)-20,24:57,61-dimethano-2,52:17,29-dimetheno-3,51,16,30-(methoxyethanoxymethino)-1H,18H,26H,28H,53H,55H-bis[1,3]benzodioxocino[9,8-*d*9',8'-*d'*]bis[1,3]benzodioxocino[9',10':17,18;10',9':25,26][1,3,6,11,14,16,19,24]octaoxacyclohexacosino[4,5-*f*:13,12-*j*]bis[1,3]benzodioxocin, Stereoisomer 5⊙NMP. Procedure C.** A mixture of diol **2** (100 mg, 0.045 mmol), 50 mL of NMP, 1 g of  $Cs_2CO_3$ , and 33 mg (0.09 mmol) of 1,2-ethanediol ditosylate was stirred at 75 °C for 24 h, and a second portion of 66 mg (0.18 mmol) of 1,2-ethanediol ditosylate was added. After stirring at 75 °C for another 24 h, the solvent was removed in vacuo and the residue was dissolved in  $CHCl_3$ . The remaining solids were filtered through a 1 cm pad of Celite and the solvent was rotary evaporated, concentrated to ~3 mL, and poured into 100 mL of methanol. The precipitate that formed was filtered and chromatographed on a preparative TLC plate with  $CHCl_3$  to give 47 mg (45%) of 5⊙NMP:  $^1H$  NMR  $\delta$  -0.93 (2 H, q); -0.89 (3 H, s); -0.72 (2 H, t); 1.99 (12 H, m); 2.51 (16 H, m); 2.67 (16 H, m); 3.95 (8 H, br s); 4.06 (4 H, br s); 4.21 (4 H, d,  $J = 7.0$  Hz); 4.42 (4 H, d,  $J = 7.0$  Hz); 4.54 (4 H, s); 4.81 (8 H, m); 6.05 (4H, d,  $J = 7.3$  Hz); 6.80 (2 H, s); 6.83 (4 H, s); 6.87 (2 H, s); 7.12 (16 H, m); 7.24 (24 H, m); FAB MS,  $m/e$  (2320.0,  $M^+$ ) 2320.2, (100). Anal. Calcd for  $C_{147}H_{141}NO_{25}$ : C, 76.05; H, 6.12. Found: C, 76.09; H, 6.06.

**5⊙DMSO.** Application of procedure C to 100 mg (0.045 mmol) of diol **2**, 15 mL of DMSO, 1 g of  $Cs_2CO_3$ , and 99 mg (0.27 mmol) of 1,2-ethanediol ditosylate gave 42 mg (41%) of 5⊙DMSO after preparative TLC:  $^1H$  NMR  $\delta$  -0.48 (6 H, s); 2.02 (12 H, br s); 2.47 (16 H, m); 2.68 (16 H, m); 3.95 (8 H, br s); 4.04 (4 H, br s); 4.12 (4 H, d,  $J = 7.1$  Hz); 4.28 (4 H, d,  $J = 7.1$  Hz); 4.54 (4 H, s); 4.84 (8 H, m); 5.86 (8 H, t,  $J = 7.6$  Hz); 6.78 (2 H, s); 6.85 (4 H, s); 6.89 (2 H, s); 7.17 (16 H, m); 7.23 (24 H, m); FAB MS,  $m/e$  (2298.9,  $M^+$ ) 2301.4 (100), 2222.8 (30). Anal. Calcd for  $C_{144}H_{138}O_{25}S$ : C, 75.18; H, 6.05. Found: C, 75.08; H, 6.05.

**5⊙DMA.** Application of procedure C to 100 mg (0.045 mmol) of diol **2**, 20 mL of DMA, 1 g of  $Cs_2CO_3$ , and 99 mg (0.27 mmol) of 1,2-ethanediol ditosylate gave 44 mg (42%) of 5⊙DMA after preparative TLC:  $^1H$  NMR  $\delta$  -1.67 (3 H, s); -0.56 (3 H, s); 1.64 (3 H, s); 1.96 (12 H, m); 2.48 (16 H, m); 2.67 (16 H, m); 3.92 (8 H, t, br s); 4.01 (4 H, br s); 4.14 (4 H, d,  $J = 7.1$  Hz); 4.45 (4 H, d,  $J = 7.1$  Hz); 4.65 (4 H, s); 4.83 (8 H, m); 5.81 (8H, t,  $J = 6.4$  Hz); 6.75 (2 H, s); 6.83 (4 H, s); 6.89 (2 H, s); 7.16 (16 H, m); 7.22 (24 H, m); FAB MS,  $m/e$  (2308.0,  $M^+$ ) 2309.7 (100). Anal. Calcd for  $C_{146}H_{141}NO_{25}$ : C, 75.92; H, 6.15. Found: C, 75.87; H, 5.96.

**5⊙1,4-Me<sub>2</sub>C<sub>6</sub>H<sub>4</sub>.** Application of procedure B to 30 mg (0.013 mmol) of 5⊙DMA and 1 mL of *p*-xylene gave after preparative TLC with  $CHCl_3$  25 mg (88%) of 5⊙1,4-Me<sub>2</sub>C<sub>6</sub>H<sub>4</sub>:  $^1H$  NMR  $\delta$  -1.93 (6 H, s); 1.21 (4 H, m); 2.10 (8 H, m); 2.52 (16 H, m); 2.70 (16 H, m); 3.09 (4 H, t); 4.03 (4 H, br s); 4.11 (4 H, d,  $J = 6.9$  Hz); 4.17 (4 H, d,  $J = 6.9$  Hz); 4.18 (4 H, s); 4.21 (4 H, t); 4.86 (8 H, m); 5.69 (4H, d,  $J = 6.9$  Hz); 5.78 (4H, d,  $J = 6.9$  Hz); 5.97 (4 H, s); 6.82 (2 H, s); 6.85 (2 H, s); 6.94 (4 H, s); 7.17 (16 H, m); 7.23 (24 H, m); FAB MS,  $m/e$  (2327.0,  $M^+$ ) 2329.7 (100), 2224.0 (90). Anal. Calcd for  $C_{150}H_{142}O_{24}$ : C, 77.37; H, 6.15. Found: C, 77.68; H, 5.98.

**8,9,10,11,39,40,41,42-Octahydro-1,18,26,28,53,55,63,79-octaphenethyl-34,47-(epoxybutanoxy)-20,24:57,61-dimethano-2,52:17,29-dimetheno-3,51,16,30-(methoxypropyloxymethino)-1H,18H,26H,28H,53H,55H-bis[1,3]benzodioxocino[9,8-*d*9',8'-*d'*]bis[1,3]benzodioxocino[9',10':17,18;10',9':25,26][1,3,6,11,14,16,19,24]octaoxacyclohexacosino[4,5-*f*:13,12-*j*]bis[1,3]benzodioxocin, Stereoisomer 6 (Empty). Procedure D.** A mixture of diol **2** (100 mg (0.045 mmol), 10 mL of HMPA, 1 g of  $Cs_2CO_3$ , and 35 mg (0.09 mmol) of 1,3-propanediol ditosylate was stirred at 75 °C for 24 h, and

70 mg (0.18 mmol) more of 1,3-propanediol ditosylate was added. After stirring at 75 °C for another 24 h, the mixture was poured into 50 mL of 5% NaCl (aq). The precipitate that formed was filtered, washed with methanol, and chromatographed on a preparative TLC plate with  $CHCl_3$  to give 46 mg (46%) of **6** (empty):  $^1H$  NMR  $\delta$  1.99 (12 H, br s); 2.22 (2 H, m); 2.51 (16 H, m); 2.67 (16 H, m); 3.90 (12 H, m); 4.18 (4 H, t,  $J = 7.1$  Hz); 4.30 (8 H, d,  $J = 7.8$  Hz); 4.81 (8 H, t,  $J = 7.8$  Hz); 5.78 (4 H, d,  $J = 7.3$  Hz); 5.82 (4 H, d,  $J = 7.3$  Hz); 6.82 (8 H, m); 7.12 (16 H, m); 7.23 (24 H, m); FAB MS,  $m/e$  (2234.9,  $M^+$ ) 2237.5 (100). Anal. Calcd for  $C_{143}H_{134}O_{24} \cdot 2H_2O$ : C, 75.57; H, 6.12. Found: C, 75.62; H, 6.09.

**6⊙NMP.** Application of procedure C to 100 mg (0.045 mmol) of diol **2**, 50 mL of NMP, 1 g of  $Cs_2CO_3$ , and 35 mg (0.09 mmol) of 1,3-propanediol ditosylate (first portion) and 70 mg (0.18 mmol) of 1,3-propanediol ditosylate (second portion) gave after preparative TLC with  $CHCl_3$  67 mg (64%) of 6⊙NMP:  $^1H$  NMR  $\delta$  -0.90 (3 H, s); -0.82 (2 H, q); -0.60 (2 H, t); 1.98 (12 H, br s); 2.22 (2 H, m); 2.48 (16 H, m); 2.65 (16 H, m); 3.98 (12 H, m); 4.18 (4 H, t,  $J = 7.1$  Hz); 4.21 (4 H, d,  $J = 7.6$  Hz); 4.41 (4 H, d,  $J = 7.6$  Hz); 4.85 (8 H, t,  $J = 7.8$  Hz); 5.81 (8 H, t,  $J = 7.3$  Hz); 6.85 (8 H, m); 7.13 (16 H, m); 7.23 (24 H, m); FAB MS,  $m/e$  (2334.0,  $M^+$ ) 2336.0 (100). Anal. Calcd for  $C_{148}H_{143}NO_{25}$ : C, 76.11; H, 6.17. Found: C, 76.17; H, 6.17.

**6⊙DMSO.** Application of procedure C to 100 mg (0.045 mmol) of diol **2**, 50 mL of DMSO, 1 g of  $Cs_2CO_3$ , and 105 mg (0.27 mmol) of 1,3-propanediol ditosylate gave 62 mg (60%) of 6⊙DMSO after preparative TLC with  $CHCl_3$ :  $^1H$  NMR  $\delta$  -0.51 (6 H, s); 2.03 (12 H, br s); 2.25 (2 H, m); 2.50 (16 H, m); 2.69 (16 H, m); 3.94 (12 H, m); 4.19 (4 H, t); 4.21 (8 H, t); 4.84 (8 H, t,  $J = 7.8$  Hz); 5.83 (4 H, d,  $J = 7.3$  Hz); 5.88 (4 H, d,  $J = 7.3$  Hz); 6.84 (8 H, m); 7.15 (16 H, m); 7.24 (24 H, m); FAB MS,  $m/e$  (2312.9,  $M^+$ ) 2315.4 (100). Anal. Calcd for  $C_{145}H_{140}O_{25}S$ : C, 75.24; H, 6.10. Found: C, 75.31; H, 6.10.

**6⊙DMA.** Application of procedure C to 100 mg (0.045 mmol) of diol **2**, 50 mL of DMA, 1 g of  $Cs_2CO_3$ , and 105 mg (0.27 mmol) of 1,3-propanediol ditosylate gave 67 mg (64%) of 6⊙DMA after preparative TLC with  $CHCl_3$ :  $^1H$  NMR  $\delta$  -1.68 (3 H, s); -0.53 (3 H, s); 2.01 (12 H, br s); 2.25 (2 H, m); 2.49 (16 H, m); 2.68 (16 H, m); 3.91 (12 H, m); 4.20 (8 H, d,  $J = 7.2$  Hz); 4.39 (4 H, d,  $J = 7.4$  Hz); 4.84 (8 H, t,  $J = 7.9$  Hz); 5.81 (4 H, d,  $J = 7.5$  Hz); 5.84 (4 H, d,  $J = 7.5$  Hz); 6.82 (2 H, s); 6.84 (4 H, s); 6.87 (2 H, s); 7.15 (16 H, m); 7.24 (24 H, m); FAB MS,  $m/e$  (2322.0,  $M^+$ ) 2323.7 (100). Anal. Calcd for  $C_{147}H_{143}NO_{25}$ : C, 75.98; H, 6.20. Found: C, 76.16; H, 6.03.

**6⊙1,4-Me<sub>2</sub>C<sub>6</sub>H<sub>4</sub>.** Application of procedure B to 30 mg (0.013 mmol) of **6** (empty) and 1 mL of *p*-xylene gave after preparative TLC with  $CHCl_3$  27 mg (90%) of 6⊙1,4-Me<sub>2</sub>C<sub>6</sub>H<sub>4</sub>:  $^1H$  NMR  $\delta$  -2.01 (6 H, s); 1.67 (4 H, br s); 1.97 (2 H, m); 2.09 (8 H, br s); 2.52 (16 H, m); 2.70 (16 H, m); 3.36 (4 H, t,  $J = 6.9$  Hz); 3.66 (4 H, br s); 4.12 (8 H, hidden); 4.12 (4 H, d,  $J = 6.9$  Hz); 4.18 (4 H, d,  $J = 6.9$  Hz); 4.87 (8 H, t,  $J = 7.8$  Hz); 5.71 (8 H, dd,  $J = 7.0$  Hz); 5.94 (4H, s); 6.85 (4 H, s); 6.94 (4 H, s); 7.16 (16 H, m); 7.23 (24 H, m); FAB MS,  $m/e$  (2341.0,  $M^+$ ) 2342 (100), 2236 (50). Anal. Calcd for  $C_{151}H_{144}O_{24}$ : C, 77.41; H, 6.20. Found: C, 77.29; H, 6.12.

**8,9,10,11,40,41,42,43-Octahydro-1,18,26,28,54,56,64,81-octaphenethyl-34,48-(epoxybutanoxy)-20,24:58,62-dimethano-2,53:17,29-dimetheno-3,52,16,30-(methoxybutanoxymethino)-1H,18H,26H,28H,39H,54H,56H-bis[1,3]benzodioxocino[9,8-*d*9',8'-*d'*]bis[1,3]benzodioxocino[9',10':4,5;10',9':12,13][1,3,6,11,14,16,19,25]octaoxacycloheptacosino[17,18-*f*:27,26-*j*]bis[1,3]benzodioxocin, Stereoisomer 8⊙CHCl<sub>3</sub>.** A mixture of 100 mg (0.045 mmol) of diol **2**, 50 mL of NMP, 1 g of  $Cs_2CO_3$ , and 36 mg (0.09 mmol) of 1,5-pentanediol dimesylate was stirred at 25 °C for 5 h, and then the temperature was raised to 50 °C and the mixture stirred for 24 h. The solution was stirred for another 24 h after the addition of 36 mg (0.09 mmol) of 1,5-pentanediol dimesylate. The product was isolated as in procedure A to give after preparative TLC with  $CHCl_3$  81 mg (79%) of 8⊙CHCl<sub>3</sub>:  $^1H$  NMR  $\delta$  1.82 (6 H, m); 1.97 (12 H, br s); 2.49 (16 H, m); 2.68 (16 H, m); 3.88 (4 H, m); 3.97 (12 H, br s); 4.20 (4 H, d,  $J = 7.0$  Hz); 4.23 (4 H, d,  $J = 7.0$  Hz); 4.83 (8 H, m); 5.81 (4 H, d,  $J = 6.9$  Hz); 5.86 (4 H, d,  $J = 6.9$  Hz); 6.80 (2 H, s); 6.82 (2 H, s); 6.84 (4 H, s); 7.17 (16 H, m); 7.23 (24 H, m); FAB

MS,  $m/e$  (2380.9,  $M^+$ ), 2384.0 (100), 2264.6 (98). Anal. Calcd for  $C_{146}H_{139}Cl_3O_{24}$ : C, 73.56; H, 5.88. Found: C, 73.58; H, 5.60.

**8⊙CHCl<sub>2</sub>CHCl<sub>2</sub>.** Application of procedure B to 30 mg (0.013 mmol) of **8⊙CHCl<sub>3</sub>** and 1 mL of tetrachloroethane gave after preparative TLC with  $CHCl_3$  28 mg (92%) of **8⊙CHCl<sub>2</sub>-CHCl<sub>2</sub>**:  $^1H$  NMR  $\delta$  1.80 (6 H, m); 1.97 (12 H, br s); 2.49 (16 H, m); 2.69 (16 H, m); 3.88 (4 H, m); 3.98 (12 H, br s); 4.29 (2 H, s); 4.35 (8 H, dd); 4.82 (8 H, m); 5.78 (4 H, d,  $J = 7.1$  Hz); 5.83 (4 H, d,  $J = 7.1$  Hz); 6.79 (2 H, s); 6.82 (2 H, s); 6.84 (4 H, s); 7.17 (16 H, m); 7.22 (24 H, m); FAB MS,  $m/e$  (2428.8,  $M^+$ ), 2431 (100), 2263 (60). Anal. Calcd for  $C_{147}H_{140}Cl_4O_{24} \cdot 3H_2O$ : C, 71.01; H, 5.92. Found: C, 70.74; H, 5.74.

**8⊙1,4-(MeO)<sub>2</sub>C<sub>6</sub>H<sub>4</sub>.** Procedure F. Into a Pyrex test tube capped with a rubber septum were placed 30 mg (0.013 mmol) of **8⊙CHCl<sub>3</sub>**, 180 mg of 1,4-dimethoxybenzene (1.3 mmol), and 1 mL of  $Ph_2O$ . This mixture was heated at 165 °C for 3 d and poured into 50 mL of methanol. The precipitate that formed was filtered (without further purification) to give 28 mg (90%) of **8⊙1,4-(MeO)<sub>2</sub>C<sub>6</sub>H<sub>4</sub>**:  $^1H$  NMR  $\delta$  -0.41 (6 H, s); 1.56 (6 H, br s); 1.81 (8 H, br s); 2.03 (4 H, br s); 2.50 (16 H, m); 2.69 (16 H, m); 3.58 (4 H, m); 3.62 (4 H, m); 4.04 (4 H, br s); 4.08 (4 H, br s); 4.28 (8 H, t,  $J = 7.1$  Hz); 4.90 (8 H, t,  $J = 7.7$  Hz); 5.74 (8 H, t,  $J = 7.0$  Hz); 5.84 (4 H); 6.82 (4 H, s); 6.85 (2 H, s); 6.86 (2 H, s); 7.17 (16 H, m); 7.24 (24 H, m); FAB MS,  $m/e$  (2401.0,  $M^+$ ), 2402.6 (100). Anal. Calcd for  $C_{153}H_{148}O_{26} \cdot H_2O$ : C, 75.91; H, 6.25. Found: C, 76.10; H, 5.90.

**8⊙1,3-(MeO)<sub>2</sub>C<sub>6</sub>H<sub>4</sub>.** Procedure G. Into a Pyrex test tube capped with a rubber septum were placed 30 mg (0.013 mmol) of **8⊙CHCl<sub>3</sub>** and 1 mL of 1,3-dimethoxybenzene. This mixture was heated at 165 °C for 3 d and poured into 50 mL of methanol. The precipitate that formed was filtered and chromatographed on a preparative TLC plate with  $CHCl_3$  to give 28 mg (89%) of **8⊙1,3-(MeO)<sub>2</sub>C<sub>6</sub>H<sub>4</sub>**:  $^1H$  NMR  $\delta$  -0.55 (6 H, s); 1.53 (6 H, br s); 1.87 (8 H, br s); 2.03 (4 H, br s); 2.50 (16 H, m); 2.70 (16 H, m); 3.55 (4 H, m); 3.60 (4 H, m); 4.09 (8 H, br s); 4.33 (8 H, t,  $J = 6.3$  Hz); 4.92 (8 H, m); 5.02 (2 H, d); 5.48 (1 H, s); 5.74 (8 H, t,  $J = 6.0$  Hz); 6.82 (4 H, s); 6.86 (2 H, s); 6.92 (2 H, s); 7.18 (16 H, m); 7.24 (24 H, m); FAB MS,  $m/e$  (2401.0,  $M^+$ ), 2402.6 (100). Anal. Calcd for  $C_{153}H_{148}O_{26}$ : C, 76.48; H, 6.21. Found: C, 76.31; H, 6.05.

**8⊙1,2-(MeO)<sub>2</sub>C<sub>6</sub>H<sub>4</sub>.** Application of procedure G to **8⊙CHCl<sub>3</sub>** (30 mg, 0.013 mmol) and 1 mL of 1,2-(MeO)<sub>2</sub>C<sub>6</sub>H<sub>4</sub> gave, after preparative TLC with  $CHCl_3$ , 26 mg (86%) of **8⊙1,2-(MeO)<sub>2</sub>C<sub>6</sub>H<sub>4</sub>**:  $^1H$  NMR  $\delta$  1.62 (8 H, br s); 1.78 (6 H, br s); 2.04 (4 H, br s); 2.50 (16 H, m); 2.68 (16 H, m); 3.60 (4 H, br s); 3.71 (4 H, m); 4.05 (8 H, br s); 4.34 (8 H, t); 4.83 (8 H, m); 5.46 (2 H, br s); 5.70 (8 H, t,  $J = 7.0$  Hz); 6.87 (4 H, s); 6.91 (2 H, s); 6.93 (2 H, s); 7.17 (16 H, m); 7.23 (24 H, m); FAB MS  $m/e$  (2401.0,  $M^+$ ), 2401.1 (100). Anal. Calcd for  $C_{153}H_{148}O_{26}$ : C, 76.48; H, 6.21. Found: C, 76.31; H, 6.05.

**8⊙Naphthalene.** Application of procedure G to 30 mg (0.013 mmol) of **8⊙CHCl<sub>3</sub>**, 166 mg of naphthalene (1.3 mmol), and 1.5 mL of  $Ph_2O$  gave, after preparative TLC with  $CHCl_3$ , 26 mg (84%) of **8⊙naphthalene**:  $^1H$  NMR  $\delta$  1.31 (8 H, m); 1.85-2.10 (6 H, m); 2.21 (4 H, br s); 2.55 (16 H, m); 2.71 (16 H, m); 3.15 (4 H, m); 3.21 (4 H, m); 3.36 (4 H, br s); 4.21 (4 H, br s); 4.21 (4 H, br s); 4.31 (8 H, t,  $J = 7.2$  Hz); 4.88 (8 H, t,  $J = 7.7$  Hz); 5.62 (8 H, dd,  $J = 7.0$  Hz); 6.93 (4 H, s); 7.09 (2 H, s); 7.11 (2 H, s); 7.17 (16 H, m); 7.24 (24 H, m); FAB MS  $m/e$  (2391.0,  $M^+$ ), 2391.8 (100), 2265.5 (80). Anal. Calcd for  $C_{155}H_{146}O_{24}$ : C, 77.80; H, 6.15. Found: C, 78.10; H, 6.29.

**8⊙4-MeC<sub>6</sub>H<sub>4</sub>OMe.** Application of procedure G to 30 mg (0.013 mmol) of **8⊙CHCl<sub>3</sub>** and 1 mL of 4-MeC<sub>6</sub>H<sub>4</sub>OMe gave 29 mg (92%) of **8⊙4-MeC<sub>6</sub>H<sub>4</sub>OMe**:  $^1H$  NMR  $\delta$  -1.98 (3 H, s); -0.28 (3 H, s); 1.63 (8 H, br s); 1.84 (6 H, br s); 2.04 (4 H, br s); 2.52 (16 H, m); 2.69 (16 H, m); 3.46 (2 H, m); 3.59 (2 H, m); 3.70 (4 H, br s); 4.04 (8 H, br s); 4.14 (2 H, d,  $J = 7.0$  Hz); 4.16 (2 H, d,  $J = 7.0$  Hz); 4.22 (2 H, d,  $J = 7.0$  Hz); 4.29 (2 H, d,  $J = 7.0$  Hz); 4.88 (8 H, m); 5.69 (2 H, d,  $J = 6.9$  Hz); 5.71 (2 H, d,  $J = 6.9$  Hz); 5.73 (2 H, d,  $J = 6.9$  Hz); 5.78 (2 H, d,  $J = 6.9$  Hz); 5.84 (2 H, d,  $J = 8.5$  Hz); 5.95 (2 H, d,  $J = 8.5$  Hz); 6.85 (4 H, d,  $J = 8.1$  Hz); 6.87 (2 H, d,  $J = 4.0$  Hz); 6.92 (2 H, d,  $J = 4.0$  Hz); 7.17 (16 H, m); 7.24 (24 H, m); FAB MS  $m/e$  (2385.0,  $M^+$ ), 2386.3 (100), 2265.5 (40). Anal. Calcd for  $C_{153}H_{148}O_{25}$ : C, 76.99; H, 6.25. Found: C, 77.16; H, 6.24.

**8⊙2-HOC<sub>6</sub>H<sub>4</sub>Me.** Application of procedure G to 30 mg (0.013 mmol) of **8⊙CHCl<sub>3</sub>** and 1 mL of *o*-cresol gave, after preparative TLC with  $CHCl_3$ , 28 mg (90%) of **8⊙2-HOC<sub>6</sub>H<sub>4</sub>-Me**:  $^1H$  NMR  $\delta$  -1.68 (3 H, s); 1.68-2.04 (18 H, m); 2.51 (16 H, m); 2.69 (16 H, m); 3.22 (1 H, t); 3.68-4.10 (16 H, m); 4.15 (2 H, d,  $J = 7.1$  Hz); 4.29 (4 H, d,  $J = 7.7$  Hz); 4.36 (2 H, d,  $J = 7.1$  Hz); 4.84 (8 H, m); 5.63 (2 H, d,  $J = 7.1$  Hz); 5.73 (2 H, d,  $J = 7.1$  Hz); 5.78 (2 H, d,  $J = 7.0$  Hz); 5.83 (2 H, d,  $J = 7.0$  Hz); 5.98 (2 H, d); 6.14 (2 H, d); 6.21 (2 H, s); 6.71-7.08 (8 H, m); 7.17 (16 H, m); 7.23 (24 H, m); FAB MS  $m/e$  (2371.0,  $M^+$ ) 2372, (100), 2265 (80). Anal. Calcd for  $C_{152}H_{146}O_{25}$ : C, 76.94; H, 6.20. Found: C, 76.98; H, 6.23.

**6,34,35,36,37,65-Hexahydro-13,21,23,48,50,76,84-octaphenethyl-29,42-(epoxybutanoxy)-15,19:52,56-dimethano-12,24:47,59-dimetheno-11,25,46,60-(methoxybutanoxymethyno)-13H,21H,23H,48H,50H,58H-bis[1,3]-benzodioxocino[9',10':4,5;10'',9'':12,13]bis[1,3]benzodioxocino[9'',8'':4',5'][[1,3]benzodioxocino[9',10':17,18;10'',9'':25,26][1,3,6,11,14,16,19,24]octaoxacyclohexacosino[8,9-*b*]quinoxaline, Stereoisomer 9⊙NMP.** Procedure E. A mixture of 100 mg (0.045 mmol) of diol **2**, 50 mL of NMP, 1 g of  $Cs_2CO_3$ , and 20 mg (0.09 mmol) of 2,3-bis(bromomethyl)quinoxaline was stirred at 25 °C for 5 h, and then the temperature was raised to 50 °C and the mixture was stirred for 24 h. The solution was stirred for another 24 h after the addition of 20 mg (0.09 mmol) of 2,3-bis(bromomethyl)quinoxaline. The remaining solids were filtered through a 1 cm pad of Celite, and the solvent was rotary evaporated and concentrated to ~3 mL and poured into 100 mL of methanol. The precipitate that formed was filtered and chromatographed on a preparative TLC plate with  $CHCl_3$  to give 86 mg (78%) of **9⊙NMP**:  $^1H$  NMR  $\delta$  -1.17 (3 H, s); -1.15 (2 H, q); -0.96 (2 H, t); 1.80 (2 H, t); 1.97 (12 H, m); 2.47 (16 H, m); 2.66 (16 H, m); 3.92 (12 H, br s); 4.14 (4 H, d,  $J = 7.3$  Hz); 4.38 (4 H, d,  $J = 7.3$  Hz); 4.71 (4 H, t,  $J = 7.7$  Hz); 4.82 (4 H, t,  $J = 7.7$  Hz); 5.44 (4 H, s); 5.76 (8 H, d,  $J = 7.2$  Hz); 6.81 (4 H, s); 6.84 (2 H, s); 6.93 (2 H, s); 7.15 (16 H, m); 7.23 (24 H, m); 7.77 (2 H, m); 8.08 (2 H, m); FAB MS,  $m/e$  (2448.0,  $M^+$ ), 2450.7 (100), 2351.0 (60). Anal. Calcd for  $C_{155}H_{145}N_3O_{25}$ : C, 75.99; H, 5.97; N, 1.72. Found: C, 76.09; H, 6.13; N, 1.63.

**9⊙DMSO.** Application of procedure E to 100 mg (0.045 mmol) of diol **2**, 50 mL of DMSO, 1 g of  $Cs_2CO_3$ , and 40 mg (0.18 mmol) of 2,3-bis(bromomethyl)quinoxaline gave 79 mg (72%) of **9⊙DMSO** after preparative TLC ( $CHCl_3$ ):  $^1H$  NMR  $\delta$  -0.71 (6 H, s); 2.03 (12 H, m); 2.46 (16 H, m); 2.67 (16 H, m); 3.86 (12 H, m); 4.11 (4 H, d,  $J = 7.4$  Hz); 4.15 (4 H, d,  $J = 7.4$  Hz); 4.50 (4 H, t,  $J = 7.6$  Hz); 4.82 (4 H, t,  $J = 7.6$  Hz); 5.43 (4 H, s); 5.78 (4 H, d,  $J = 7.5$  Hz); 5.82 (4 H, d,  $J = 7.5$  Hz); 6.80 (4 H, s); 6.85 (2 H, s); 6.91 (2 H, s); 7.14 (16 H, m); 7.24 (24 H, m); 7.79 (2 H, m); 8.13 (2 H, m); FAB MS,  $m/e$  (2427.0,  $M^+$ ), 2430.1 (100), 2351.2 (50). Anal. Calcd for  $C_{152}H_{142}N_2O_{25}S$ : C, 75.17; H, 5.89. Found: C, 74.95; H, 6.13.

**9⊙1,4-(MeO)<sub>2</sub>C<sub>6</sub>H<sub>4</sub>.** Application of procedure D to 100 mg (0.045 mmol) of diol **2**, 10 mL of HMPA, 1 g of  $Cs_2CO_3$ , 620 mg (4.5 mmol) of 1,4-dimethoxybenzene, 20 mg (0.09 mmol) of 2,3-bis(bromomethyl)quinoxaline, and an additional 20 mg (0.09 mmol) of 2,3-bis(bromomethyl)quinoxaline (maximum temperature 50 °C) gave after preparative TLC with  $CHCl_3$  38 mg (34%) of **9⊙1,4-(MeO)<sub>2</sub>C<sub>6</sub>H<sub>4</sub>**:  $^1H$  NMR  $\delta$  -0.45 (6 H, s); 1.08 (4 H, m); 2.05 (8 H, m); 2.51 (16 H, m); 2.71 (16 H, m); 3.12 (4 H, m); 4.01 (4 H, m); 4.05 (4 H, d,  $J = 7.0$  Hz); 4.21 (4 H, m); 4.39 (4 H, d,  $J = 7.0$  Hz); 4.78 (4 H, t,  $J = 7.7$  Hz); 4.93 (4 H, t,  $J = 7.7$  Hz); 5.24 (4 H, s); 5.59 (4 H, d,  $J = 6.9$  Hz); 5.76 (4 H, d,  $J = 6.9$  Hz); 5.81 (4 H, s); 6.81 (2 H, s); 6.84 (4 H, s); 6.88 (2 H, s); 7.17 (16 H, m); 7.23 (24 H, m); 7.73 (2 H, m); 7.96 (2 H, m); FAB MS,  $m/e$  (2487.0,  $M^+$ ), 2488.9 (100). Anal. Calcd for  $C_{158}H_{146}N_2O_{26}$ : C, 76.25; H, 5.91. Found: C, 76.07; H, 6.05.

**61,62,63,64-Tetrahydro-6,14,16,44,46,54,75,84-octaphenethyl-33H,22,38-(epoxybutanoxy)-8,12:48,52-dimethano-5,17:28,32:43,55-trimetheno-4,18,42,56-(methoxybutanoxymethyno)-6H,14H,16H,27H,42H,46H,54H-bis[1,3]-benzodioxocino[9,8-*d*:9',8'-*d'*]bis[1,3]benzodioxocino[9',10':4,5;10'',9'':12,13][1,3,6,11,14,16,19,27]octaoxacyclononacosino[17,18-*j*:29,28-*j'*]bis[1,3]benzodioxocin, Stereoiso-**

**mer 10**⊙CHCl<sub>3</sub>. Application of procedure E to 100 mg (0.045 mmol) of diol **2**, 50 mL of NMP, 1 g of Cs<sub>2</sub>CO<sub>3</sub>, 16 mg (0.09 mmol) of 1,3-bis(chloromethyl)benzene, and 16 mg (0.09 mmol) of additional dichloride gave after preparative TLC with CHCl<sub>3</sub>: 88 mg (81%) of **10**⊙CHCl<sub>3</sub>: <sup>1</sup>H NMR δ 1.94 (12 H, m); 2.48 (16 H, m); 2.68 (16 H, m); 3.86 (4 H, br s); 3.96 (4 H, br s); 4.04 (4 H, br s); 4.24 (8 H, t, *J* = 7.5 Hz); 4.85 (8 H, t, *J* = 7.8 Hz); 5.06 (4 H, s); 5.73 (4 H, d, *J* = 7.1 Hz); 5.89 (4 H, d, *J* = 7.1 Hz); 6.82 (2 H, s); 6.87 (6 H, s); 7.03 (2 H, d); 7.17 (16 H, m); 7.23 (24 H, m); 7.74 (1 H, s); FAB MS *m/e* (2414.9, M<sup>+</sup>) 2419 (40), 2299 (100). Anal. Calcd for C<sub>149</sub>H<sub>137</sub>Cl<sub>3</sub>O<sub>24</sub>: C, 74.01; H, 5.71. Found: C, 73.76; H, 5.78.

**10**⊙CHCl<sub>2</sub>CHCl<sub>2</sub>. Application of procedure B to 30 mg (0.013 mmol) of **10**⊙CHCl<sub>3</sub> and 1 mL of tetrachloroethane gave after preparative TLC with CHCl<sub>3</sub> 29 mg (91%) of **10**⊙CHCl<sub>2</sub>CHCl<sub>2</sub>: <sup>1</sup>H NMR δ 1.93 (12 H, m); 2.51 (16 H, m); 2.69 (16 H, m); 3.87 (4 H, br s); 3.97 (4 H, br s); 4.03 (4 H, br s); 4.35 (2 H, s); 4.38 (8 H, t, *J* = 7.5 Hz); 4.84 (8 H, t, *J* = 7.8 Hz); 5.04 (4 H, s); 5.69 (4 H, d, *J* = 7.0 Hz); 5.84 (4 H, d, *J* = 7.0 Hz); 6.83 (2 H, s); 6.86 (6 H, s); 7.05 (2 H, d, *J* = 7.3 Hz); 7.17 (16 H, m); 7.23 (24 H, m); 7.73 (1 H, s); FAB MS *m/e* (2462.8, M<sup>+</sup>) 2466 (100), 2298 (90). Anal. Calcd for C<sub>150</sub>H<sub>138</sub>Cl<sub>4</sub>O<sub>24</sub>: C, 73.04; H, 5.64. Found: C, 73.36; H, 5.38.

**10**⊙1,4-(MeO)<sub>2</sub>C<sub>6</sub>H<sub>4</sub>. Application of procedure G to 30 mg (0.013 mmol) of **10**⊙CHCl<sub>3</sub>, 180 mg of 1,4-dimethoxybenzene (1.3 mmol), and 1 mL of Ph<sub>2</sub>O gave 28 mg (90%) of **10**⊙1,4-(MeO)<sub>2</sub>C<sub>6</sub>H<sub>4</sub>: <sup>1</sup>H NMR δ -0.38 (6 H, s); 1.49 (8 H, br s); 2.05 (4 H, br s); 2.53 (16 H, m); 2.71 (16 H, m); 3.55 (4 H, br s); 3.58 (4 H, br s); 4.09 (4 H, br s); 4.25 (4 H, d, *J* = 7.0 Hz); 4.27 (4 H, d, *J* = 7.0 Hz); 4.91 (8 H, t); 5.10 (4 H, s); 5.68 (4 H, d, *J* = 6.9 Hz); 5.73 (4 H, d, *J* = 6.9 Hz); 5.84 (4 H, s); 6.84 (4 H, s); 6.88 (2 H, s); 6.91 (2 H, s); 7.19 (16 H, m); 7.24 (24 H, m); 7.32 (2 H, d, *J* = 7.6 Hz); 7.69 (1 H, s); FAB MS *m/e* (2435.0, M<sup>+</sup>) 2435 (100). Anal. Calcd for C<sub>156</sub>H<sub>146</sub>O<sub>26</sub>: C, 76.89; H, 6.04. Found: C, 76.98; H, 6.00.

**10**⊙1,3-(MeO)<sub>2</sub>C<sub>6</sub>H<sub>4</sub>. Application of procedure F to 30 mg (0.013 mmol) of **10**⊙CHCl<sub>3</sub> and 1 mL of 1,3-dimethoxybenzene gave after preparative TLC with CHCl<sub>3</sub>, 27 mg (89%) of **10**⊙1,3-(MeO)<sub>2</sub>C<sub>6</sub>H<sub>4</sub>: <sup>1</sup>H NMR δ -0.53 (6 H, s); 1.45 (8 H, br s); 2.05 (4 H, br s); 2.53 (16 H, m); 2.72 (16 H, m); 3.49 (4 H, br s); 3.55 (4 H, br s); 4.08 (4 H, br s); 4.29 (8 H, d, *J* = 6.8 Hz); 4.91 (8 H, t); 5.03 (2 H, d); 5.13 (4 H, s); 5.48 (1 H, s); 5.66 (4 H, d, *J* = 7.0 Hz); 5.73 (4 H, d, *J* = 6.9 Hz); 6.83 (4 H, s); 6.89 (2 H, s); 6.93 (2 H, s); 7.19 (16 H, m); 7.24 (24 H, m); 7.43 (1 H, t); 7.78 (1 H, s); FAB MS *m/e* (2435.0, M<sup>+</sup>) 2436 (100). Anal. Calcd for C<sub>156</sub>H<sub>146</sub>O<sub>26</sub>: C, 76.89; H, 6.04. Found: C, 76.66; H, 6.23.

**10**⊙1,2-(MeO)<sub>2</sub>C<sub>6</sub>H<sub>4</sub>. Application of procedure F to 30 mg (0.013 mmol) of **10**⊙CHCl<sub>3</sub> and 1 mL of 1,2-(MeO)<sub>2</sub>C<sub>6</sub>H<sub>4</sub> gave after preparative TLC with CHCl<sub>3</sub>, 27 mg (87%) of **10**⊙1,2-(MeO)<sub>2</sub>C<sub>6</sub>H<sub>4</sub>: <sup>1</sup>H NMR δ 1.59 (8 H, br s); 2.03 (4 H, br s); 2.50 (16 H, m); 2.68 (16 H, m); 3.58 (4 H, br s); 3.69 (4 H, m); 4.08 (4 H, br s); 4.30 (8 H, t, *J* = 7.5 Hz); 4.88 (8 H, m); 5.12 (4 H, s); 5.45 (2 H, br s); 5.71 (8 H, d, *J* = 7.8 Hz); 6.89 (4 H, s); 6.99 (2 H, s); 7.01 (2 H, s); 7.18 (16 H, m); 7.24 (24 H, m); 7.34 (2 H, d); 7.51 (1 H, t); 7.71 (1 H, s); FAB MS *m/e* (2435.0, M<sup>+</sup>) 2436 (100). Anal. Calcd for C<sub>156</sub>H<sub>146</sub>O<sub>26</sub>: C, 76.89; H, 6.04. Found: C, 76.62; H, 6.09.

**10**⊙Naphthalene. Application of procedure G to 30 mg (0.013 mmol) of **10**⊙CHCl<sub>3</sub>, 166 mg of naphthalene (1.3 mmol), and 1.5 mL of Ph<sub>2</sub>O gave after preparative TLC with CHCl<sub>3</sub> 27 mg (85%) of **10**⊙naphthalene: <sup>1</sup>H NMR δ 1.31 (8 H, m); 2.20 (4 H, m); 2.56 (16 H, m); 2.71 (16 H, m); 3.12 (4 H, m); 3.21 (4 H, m); 3.35 (4 H, m); 4.19 (4 H, br s); 4.30 (4 H, d, *J* = 7.1 Hz); 4.34 (4 H, d, *J* = 7.1 Hz); 4.89 (8 H, m); 5.21 (4 H, s); 5.54 (4 H, d, *J* = 6.9 Hz); 5.61 (4 H, d, *J* = 6.9 Hz); 6.98 (4 H, s); 7.12 (2 H, s); 7.18 (16 H, m); 7.24 (24 H, m); 7.41 (1 H, t); 8.08 (1 H, s); FAB MS *m/e* (2425.0, M<sup>+</sup>) 2425.1 (100). Anal. Calcd for C<sub>158</sub>H<sub>144</sub>O<sub>24</sub>·2H<sub>2</sub>O: C, 77.05; H, 6.06. Found: C, 77.04; H, 5.95.

**10**⊙4-MeC<sub>6</sub>H<sub>4</sub>OMe. Application of procedure F to 30 mg (0.013 mmol) of **10**⊙CHCl<sub>3</sub> and 1 mL of 4-MeC<sub>6</sub>H<sub>4</sub>OMe gave 28 mg (90%) of **10**⊙4-MeC<sub>6</sub>H<sub>4</sub>OMe: <sup>1</sup>H NMR δ -1.96 (3 H, s); -0.26 (3 H, s); 1.58 (8 H, br s); 2.03 (4 H, br s); 2.50 (16 H, m); 2.69 (16 H, m); 3.39 (2 H, m); 3.58 (2 H, m); 3.62 (2 H, m); 3.71 (2 H, m); 4.02 (4 H, br s); 4.16 (2 H, d, *J* = 7.0 Hz); 4.18

(2 H, d, *J* = 7.0 Hz); 4.22 (2 H, d, *J* = 7.0 Hz); 4.29 (2 H, d, *J* = 7.0 Hz); 4.89 (8 H, m); 5.62 (4 H, d, *J* = 8.4 Hz); 5.62 (4 H, t, *J* = 6.8 Hz); 5.73 (2 H, d, *J* = 6.9 Hz); 5.80 (2 H, d, *J* = 6.9 Hz); 5.87 (2 H, d, *J* = 8.5 Hz); 6.01 (2 H, d, *J* = 8.5 Hz); 6.80–7.01 (8 H, m); 7.17 (16 H, m); 7.24 (24 H, m); 7.38 (1 H, t); 7.80 (1 H, s); FAB MS *m/e* (2419.0, M<sup>+</sup>) 2419.9 (100). Anal. Calcd for C<sub>156</sub>H<sub>146</sub>O<sub>25</sub>: C, 77.40; H, 6.08. Found: C, 77.71; H, 6.26.

**10**⊙1,2,3-(MeO)<sub>3</sub>C<sub>6</sub>H<sub>3</sub>. Application of procedure F to 30 mg (0.013 mmol) of **10**⊙CHCl<sub>3</sub>, 220 mg of 1,2,3-trimethoxybenzene (1.3 mmol), and 1 mL of Ph<sub>2</sub>O gave after preparative TLC with CHCl<sub>3</sub> 26 mg (80%) of **10**⊙1,2,3-(MeO)<sub>3</sub>C<sub>6</sub>H<sub>3</sub>: <sup>1</sup>H NMR δ -0.41 (6 H, s); 1.45 (8 H, br s); 2.08 (4 H, br s); 2.51 (16 H, m); 2.71 (16 H, m); 3.05 (3 H, s); 3.62 (8 H, br s); 4.12 (4 H, br s); 4.39 (4 H, d, *J* = 7.2 Hz); 4.49 (4 H, d, *J* = 7.2 Hz); 4.92 (8 H, m); 5.18 (4 H, s); 5.67 (4 H, d, *J* = 6.9 Hz); 5.73 (4 H, d, *J* = 6.9 Hz); 6.86 (4 H, s); 6.90 (2 H, s); 6.98 (2 H, s); 7.18 (16 H, m); 7.24 (24 H, m); 7.34 (2 H, d); 7.46 (1 H, t); 7.60 (1 H, s); FAB MS *m/e* (2465.0, M<sup>+</sup>) 2468.3 (100). Anal. Calcd for C<sub>157</sub>H<sub>148</sub>O<sub>27</sub>: C, 76.44; H, 6.05. Found: C, 76.26; H, 5.94.

**61,62,63,64-Tetrahydro-6,14,16,44,46,54,75,84-octaphenethyl-33H-22,38-(epoxybutanoxo)-8,12:48,52-dimethano-5,17:43,55-dimetheno-4,18,42,56-(methoxybutanoxo-metheno)-28,32-nitrilo-6H,14H,16H,27H,44H,46H,54H-bis-[1,3]benzodioxocino[9,8-*d*'9',8'-*d*']bis[1,3]benzodioxocino[9',10':4,5;10'',9'':12,13][1,3,6,11,14,16,19,27]octaoxacyclonacosino[17,18-*j*29,28-*j*']bis[1,3]benzodioxocin, Stereoisomer 11**⊙CHCl<sub>3</sub>. A mixture of 100 mg (0.045 mmol) of diol **2**, 50 mL of NMP, 1 g of Cs<sub>2</sub>CO<sub>3</sub>, and 16 mg (0.09 mmol) of 2,6-bis(chloromethyl)pyridine was stirred at 25 °C for 5 h, and then the temperature was raised to 50 °C and the mixture stirred for 24 h. The solution was stirred for another 24 h after the addition of 16 mg (0.09 mmol) of 2,6-bis(chloromethyl)pyridine. The solvent was removed in vacuo, and the residue was dissolved in CHCl<sub>3</sub>. The remaining solids were filtered through a 1 cm pad of Celite, and the filtrate was rotary evaporated, concentrated to ~3 mL, and poured into 100 mL of methanol. The precipitate that formed was filtered and chromatographed on a preparative TLC plate with CHCl<sub>3</sub> to give 84 mg (77%) of **11**⊙CHCl<sub>3</sub>: <sup>1</sup>H NMR δ 1.91 (8 H, m); 1.98 (4 H, m); 2.49 (16 H, m); 2.69 (16 H, m); 3.87 (4 H, m); 3.90 (4 H, m); 3.98 (4 H, br s); 4.20 (4 H, d); 4.32 (4 H, d); 4.83 (8 H, m); 5.12 (4 H, s); 5.62 (4 H, d, *J* = 6.2 Hz); 5.82 (4 H, d, *J* = 6.2 Hz); 6.81 (2 H, s); 6.83 (4 H, s); 6.88 (2 H, s); 7.03 (2 H, d); 7.17 (16 H, m); 7.24 (24 H, m); 7.35 (1 H, br s); FAB MS *m/e* (2415.9, M<sup>+</sup>) 2420 (100), 2300 (25). Anal. Calcd for C<sub>148</sub>H<sub>136</sub>Cl<sub>3</sub>NO<sub>24</sub>: C, 73.48; H, 5.78. Found: C, 73.22; H, 5.57.

**11**⊙Naphthalene. Application of procedure F to 30 mg (0.013 mmol) of **11**⊙CHCl<sub>3</sub>, 166 mg of naphthalene (1.3 mmol), and 1.5 mL of Ph<sub>2</sub>O gave after preparative TLC with CHCl<sub>3</sub> 27 mg (87%) of **11**⊙naphthalene: <sup>1</sup>H NMR δ 1.20 (8 H, m); 2.19 (4 H, m); 2.57 (16 H, m); 2.71 (16 H, m); 3.12 (8 H, m); 3.37 (4 H, m); 4.19 (4 H, br s); 4.20 (4 H, d, *J* = 7.0 Hz); 4.30 (4 H, d, *J* = 7.0 Hz); 4.87 (8 H, m); 5.38 (4 H, s); 5.53 (4 H, d, *J* = 6.9 Hz); 5.58 (4 H, d, *J* = 6.9 Hz); 6.94 (4 H, s); 7.12 (2 H, s); 7.18 (16 H, m); 7.24 (24 H, m); 7.64 (1 H, t); FAB MS *m/e* (2426.0, M<sup>+</sup>) 2427.9 (100), 2300.5 (80). Anal. Calcd for C<sub>157</sub>H<sub>143</sub>NO<sub>24</sub>: C, 77.67; H, 5.94. Found: C, 77.29; H, 5.83.

**11**⊙1,2-(MeO)<sub>2</sub>C<sub>6</sub>H<sub>4</sub>. Application of procedure F to 30 mg (0.013 mmol) of **11**⊙CHCl<sub>3</sub> and 1 mL of 1,2-(MeO)<sub>2</sub>C<sub>6</sub>H<sub>4</sub> gave after preparative TLC with CHCl<sub>3</sub> 27 mg (84%) of **11**⊙1,2-(MeO)<sub>2</sub>C<sub>6</sub>H<sub>4</sub>: <sup>1</sup>H NMR δ 1.58 (8 H, br s); 2.05 (4 H, br s); 2.53 (16 H, m); 2.70 (16 H, m); 3.57 (4 H, br s); 3.67 (4 H, m); 4.11 (4 H, br s); 4.25 (8 H, m); 4.87 (8 H, m); 5.27 (4 H, s); 5.55 (2 H, br s); 5.69 (8 H, d, *J* = 7.0 Hz); 6.89 (4 H, s); 6.97 (2 H, s); 6.98 (2 H, s); 7.18 (16 H, m); 7.24 (24 H, m); 7.34 (2 H, d); 7.59 (1 H, br s); FAB MS *m/e* (2436.0, M<sup>+</sup>) 2438.6 (100), 2300.9 (30). Anal. Calcd for C<sub>155</sub>H<sub>145</sub>NO<sub>26</sub>: C, 76.37; H, 6.00. Found: C, 76.53; H, 5.99.

**11**⊙1,3-(MeO)<sub>2</sub>C<sub>6</sub>H<sub>4</sub>. Application of procedure F to 30 mg (0.013 mmol) of **11**⊙CHCl<sub>3</sub> and 1 mL of 1,3-dimethoxybenzene gave after preparative TLC with CHCl<sub>3</sub>, 27 mg (86%) of **11**⊙1,3-(MeO)<sub>2</sub>C<sub>6</sub>H<sub>4</sub>: <sup>1</sup>H NMR δ -0.50 (6 H, s); 1.40 (8 H, m); 2.08 (4 H, br s); 2.52 (16 H, m); 2.71 (16 H, m); 3.53 (8 H, m); 4.11 (4 H, br s); 4.35 (8 H, d, *J* = 6.8 Hz); 4.90 (8 H, t); 5.00 (2 H, d); 5.34 (4 H, s); 5.49 (1 H, s); 5.70 (8 H, d, *J* = 7.0 Hz);



6.83 (4 H, s); 6.89 (2 H, s); 6.93 (2 H, s); 7.19 (16 H, m); 7.24 (24 H, m); 7.74 (1 H, br s); FAB MS  $m/e$  (2436.0,  $M^+$ ) 2437.9 (90), 2300.4 (100). Anal. Calcd for  $C_{155}H_{145}NO_{26}$ : C, 76.37; H, 6.00. Found: C, 76.40; H, 5.98.

**11 $\odot$ 4-MeC<sub>6</sub>H<sub>4</sub>OMe.** Application of procedure F to 30 mg (0.013 mmol) of **11 $\odot$ CHCl<sub>3</sub>** and 1 mL of 4-MeC<sub>6</sub>H<sub>4</sub>OMe gave 28 mg (90%) of **11 $\odot$ 4-MeC<sub>6</sub>H<sub>4</sub>OMe**: <sup>1</sup>H NMR  $\delta$  -1.98 (3 H, s, guest CH<sub>3</sub>); -0.29 (3 H, s); 1.58 (8 H, br s); 2.02 (4 H, br s); 2.50 (16 H, m); 2.69 (16 H, m); 3.38 (2 H, m); 3.54 (2 H, m); 3.61 (2 H, m); 3.68 (2 H, m); 4.02 (4 H, br s); 4.15 (8 H, m); 4.87 (8 H, m); 5.48 (4 H, d); 5.72 (8 H, m); 5.78 (2 H, d); 5.90 (2 H, d); 6.80-7.01 (8 H, m); 7.17 (16 H, m); 7.24 (24 H, m); 7.71 (1 H, m); FAB MS  $m/e$  (2420.0,  $M^+$ ) 2421.2 (100), 2300.7 (30). Anal. Calcd for  $C_{155}H_{145}NO_{25}$ : C, 76.87; H, 6.03. Found: C, 77.13; H, 6.00.

**Kinetics of Decomplexations of 7 $\odot$ guest, 8 $\odot$ guest, and 10 $\odot$ guest in CDCl<sub>3</sub>.** Solutions of 5-7 mg of the three

hemiacarceplexes were dissolved in 0.5 mL of CDCl<sub>3</sub> at 25 °C, and changes in guest-proton spectra were monitored over the periods indicated in Table 3. The half-lives for decomplexation were calculated from the first-order rate constants for either disappearance of complexed guest and/or appearance of free guest.

**Supporting Information Available:** Details of crystallographic data collection and refinement for **8 $\odot$ 4-MeC<sub>6</sub>H<sub>4</sub>OMe $\odot$ 2C<sub>6</sub>H<sub>5</sub>NO<sub>2</sub>** and **10 $\odot$ CHCl<sub>3</sub> $\odot$ 2C<sub>6</sub>H<sub>5</sub>NO<sub>2</sub> $\odot$ 2C<sub>6</sub>H<sub>5</sub>NO<sub>2</sub>** (2 pages). This material is contained in libraries on microfiche, immediately follows this article in the microfilm version of the journal, and can be ordered from the ACS; see any current masthead page for ordering information.

JO9612786